Pergamon

Int. J. Solids Structures Vol. 32, No. 15, pp. 2219–2244, 1995

0020 7683/95 $9.50 + .00

0020–7683(94)00251–7

STEADY-STATE CREEP OF FIBER-REINFORCED COMPOSITES: CONSTITUTIVE EQUATIONS AND COMPUTATIONAL ISSUES

N. ARAVAS, CAO CHENG and P. PONTE CASTAÑEDA
Department of Mechanical Engineering and Applied Mechanics, University of Pennsylvania, Philadelphia, PA 19104, USA

(*Received* 2 *March* 1994; *in revised form* 22 *September* 1994)

Abstract—The general form of the constitutive equations that describe steady-state creep of fiber-reinforced metal-matrix composites with transversely isotropic overall symmetry is developed. The physical meaning of the constitutive functions involved is discussed in detail. A method for the numerical integration of the constitutive equations is developed. The "linearization moduli" associated with the integration algorithm are computed, and the constitutive model is implemented in a general purpose finite element program. A constitutive model for steady-state creep of fiber-reinforced composite that has been developed recently by deBotton and Ponte Castañeda (1993) is also considered. A number of "unit cell" problems with periodic boundary conditions, consistent with the requirements of homogenization theory, are solved by using the finite element method, and the results are compared with the predictions of the analytical model of deBotton and Ponte Castañeda.

1. INTRODUCTION

Fiber-reinforced metal-matrix composites are expected to play a key role in achieving the performance goals of the next generation of aircraft engines. Compared with traditional metal alloys, these materials have superior creep resistance at elevated temperatures, as well as a high strength-to-stiffness ratio.

In view of their potential as high-temperature structural materials, metal-matrix composites have attracted increasing attention recently, and various attempts to develop constitutive models for the mechanical behavior of such materials have been made. Several *one-dimensional* models that can be used to predict the creep behavior of fiber-reinforced composites under simple types of loading are already available in the literature; we mention amongst these the work of Mileiko (1970), Kelly and Street (1972), McLean (1985, 1988), Goto and McLean (1991a,b), and McMeeking (1993a,b). Johnson (1977) appears to have been the first to propose a set of *three-dimensional* constitutive equations for creeping transversely isotropic materials; he based his model for steady-state creep in directionally-solidified eutectic alloys on a generalization of the Bailey–Norton law, which connects the creep strain rate and applied stress by a power-law relation. More recently, deBotton and Ponte Castañeda (1993) have developed estimates as well as rigorous bounds for the dissipation functions of multiple-phase fiber composites, in which the constituent phases are non-linear isotropic materials. The work of deBotton and Ponte Castañeda was presented in the context of non-linear elastic materials, but it can be also used to describe the *steady-state* creep of fiber-reinforced transversely isotropic composites. A review of several models for the effect of fibers on the creep characteristics of unidirectional composites has been presented by McMeeking (1993a). It appears that, whereas some progress has been made in developing constitutive equations for creeping anisotropic composites, there have been few experimental studies on fiber-reinforced composite systems having practical utility at elevated temperatures. The creep behavior of metal-matrix composites reinforced with continuous fibers was studied recently by Weber *et al.* (1992). Their results show that, when both the matrix and the fibers creep, the composite exhibits steady-state behavior, following an initial transient; however, when the fibers do not creep, transient creep of the composite is observed, with a creep strain limited by the elastic deformation of the fibers.

In this paper, we develop the general three-dimensional form of the constitutive equations that describe steady-state creep of fiber-reinforced metal-matrix composites with transversely isotropic overall symmetry. The constitutive equations for the creep strain rate involve four scalar functions that depend on the five transversely isotropic invariants of the stress tensor; the physical meaning of these constitutive functions is discussed in detail. The numerical implementation of the general form of the transversely isotropic constitutive equations in a finite element program is discussed, and a method for the numerical integration of such equations is presented. A specific constitutive model for steady-state creep of fiber-reinforced composites that has been developed recently by deBotton and Ponte Castañeda (1993) is examined. The predictions of the model are compared with the solutions of a number of "unit cell" problems; periodic boundary conditions, consistent with the requirements of homogenization theory, are imposed on the unit cell problems, and the solutions are obtained by using the finite element method. Finally, the model of deBotton and Ponte Castañeda (1993) is implemented in a general purpose finite element program, and the problem of a composite plate with a hole is solved.

Standard notation is used throughout. Boldface symbols denote tensors, the order of which is indicated by the context. All tensor components are written with respect to a fixed Cartesian coordinate system, and the summation convention is used for repeated indices, unless otherwise indicated. The prefices tr and det indicate the trace and the determinant, respectively, a superscript T indicates the transpose of a second order tensor, a superposed dot denotes the material time derivative, and the subscripts s and a indicate the symmetric and anti-symmetric parts of a second order tensor. Let $\mathbf{a}$ and $\mathbf{b}$ be vectors, $\mathbf{A}$ and $\mathbf{B}$ second-order tensors, and $\mathbf{C}$ and $\mathbf{D}$ fourth-order tensors; the following products are used in the text: $(\mathbf{ab})_{ij} = a_i b_j$, $(\mathbf{A}\cdot\mathbf{a})_i = A_{ij}a_j$, $(\mathbf{a}\cdot\mathbf{A})_i = a_j A_{ji}$, $(\mathbf{A}\cdot\mathbf{B})_{ij} = A_{ik}B_{kj}$, $\mathbf{A}:\mathbf{B} = A_{ij}B_{ij}$, $(\partial\mathbf{A}/\partial\mathbf{B})_{ijkl} = \partial A_{ij}/\partial B_{kl}$, $(\mathbf{AB})_{ijkl} = A_{ij}B_{kl}$, $(\mathbf{C}:\mathbf{A})_{ij} = C_{ijkl}A_{kl}$, and $(\mathbf{C}:\mathbf{D})_{ijkl} = C_{ijmn}D_{mnkl}$.

2. CONSTITUTIVE EQUATIONS

We consider infinitesimal deformations and write the infinitesimal strain tensor $\boldsymbol{\varepsilon}$ as the sum of the elastic and the creep strains, i.e.

$$\boldsymbol{\varepsilon} = \boldsymbol{\varepsilon}^{e} + \boldsymbol{\varepsilon}^{cr}. \tag{1}$$

The focus of this paper is the steady-state creep behavior of fiber-reinforced composites. However, for comparison purposes, we start with a brief discussion of some commonly used constitutive equations for creeping *isotropic* materials.

2.1 *Creep of isotropic materials*

The constitutive equation for the steady-state creep strain rate is of the form

$$\dot{\boldsymbol{\varepsilon}}^{cr} = \mathbf{g}(\boldsymbol{\sigma}, s), \tag{2}$$

where $\mathbf{g}$ is an isotropic function of its arguments, $\boldsymbol{\sigma}$ is the stress tensor, and s is a set of material constants. Using the representation theorems for isotropic functions, we can readily show that the most general form of the last equation is (Wang, 1970a,b; Smith, 1971)

$$\dot{\boldsymbol{\varepsilon}}^{cr} = c_1\mathbf{I} + 2c_2\boldsymbol{\sigma} + 3c_3\boldsymbol{\sigma}^2, \tag{3}$$

where the c_is are functions of s and the three isotropic stress invariants $I_1 = \mathrm{tr}(\boldsymbol{\sigma})$, $I_2 = \mathrm{tr}(\boldsymbol{\sigma}^2)$, and $I_3 = \mathrm{tr}(\boldsymbol{\sigma}^3)$.

We assume next that the creep strain rate $\dot{\boldsymbol{\varepsilon}}^{cr}$ is derived from a creep potential $\Psi = \Psi(\boldsymbol{\sigma}, s)$, i.e.

$$\dot{\boldsymbol{\varepsilon}}^{cr} = \frac{\partial \Psi}{\partial \boldsymbol{\sigma}}. \tag{4}$$

The creep potential must be an isotropic function, i.e. a function of the form

$$\Psi = \Psi(I_1, I_2, I_3, s). \tag{5}$$

Using the chain rule, we can readily show that

$$\dot{\boldsymbol{\varepsilon}}^{cr} = \frac{\partial \Psi}{\partial \boldsymbol{\sigma}} = \sum_{i=1}^{3} \frac{\partial \Psi}{\partial I_i} \frac{\partial I_i}{\partial \boldsymbol{\sigma}} = c_1 \mathbf{I} + 2c_2 \boldsymbol{\sigma} + 3c_3 \boldsymbol{\sigma}^2, \tag{6}$$

where now

$$c_i = \frac{\partial \Psi}{\partial I_i}. \tag{7}$$

The three-dimensional form of the standard steady-state "power-law" creep constitutive equations is

$$\dot{\boldsymbol{\varepsilon}}^{cr} = \frac{\partial \Psi}{\partial \boldsymbol{\sigma}} = \tfrac{3}{2}\dot{\varepsilon}_0 \left(\frac{\sigma_e}{\sigma_0}\right)^{n-1} \frac{\boldsymbol{\sigma}'}{\sigma_0} \quad \text{where} \quad \Psi = \Psi(I_1, I_2) = \frac{\sigma_0 \dot{\varepsilon}_0}{n+1} \left(\frac{\sigma_e}{\sigma_0}\right)^{n+1}, \tag{8}$$

$\boldsymbol{\sigma}'$ is the stress deviator, $\sigma_e = (1.5\,\sigma'_{ij}\sigma'_{ij})^{1/2} = [0.5(3I_2 - I_1^2)]^{1/2}$ is the von Mises equivalent stress, n is the creep exponent, and $(\sigma_0, \dot{\varepsilon}_0)$ are material constants. Equation (8) is a special case of (3) with

$$c_1 = -\tfrac{2}{3} I_1 c_2, \quad c_2 = \frac{3}{4} \frac{\dot{\varepsilon}_0}{\sigma_0} \left(\frac{\sigma_e}{\sigma_0}\right)^{n-1}, \quad c_3 = 0. \tag{9}$$

Note that the power-law creep equation, eqn (8), does not involve a quadratic stress generator term $\boldsymbol{\sigma}^2$ (i.e. $c_3 = 0$).

2.2 *Fiber-reinforced composites*

Consider next a material reinforced by aligned fibers. The macroscopic response of the composite is assumed to be transversely isotropic, and the unit vector $\mathbf{n}$ in the direction of the fibers is used to define the axis of rotational symmetry.

2.2.1 *Elasticity.* The elastic strain is written in terms of the stress tensor $\boldsymbol{\sigma}$ as

$$\boldsymbol{\varepsilon}^e = \mathbf{C}^{-1} : \boldsymbol{\sigma}, \tag{10}$$

where $\mathbf{C}$ is the fourth-order elasticity tensor for a linear transversely isotropic material. The elasticity tensor is of the form (Aravas, 1992)

$$\mathbf{C} = 2a\mathbf{II} + 2b\mathbf{J} + 2c\mathbf{aa} + d\mathbf{P} + e(\mathbf{Ia} + \mathbf{aI}), \tag{11}$$

where $\mathbf{I}$ is the second-order identity tensor, $\mathbf{J}$ is the fourth-order identity tensor with cartesian components $J_{ijkl} = (\delta_{ik}\delta_{jl} + \delta_{il}\delta_{jk})/2$, $\mathbf{a}$ is the orientation tensor $\mathbf{a} = \mathbf{nn}$, (a, b, c, d, e) are elastic constants, and

$$P_{ijkl} = \tfrac{1}{2}(a_{ik}\delta_{jl} + a_{il}\delta_{jk} + \delta_{ik}a_{jl} + \delta_{il}a_{jk}). \tag{12}$$

The constants (a, b, c, d, e) are related to the standard elastic moduli $(E_{11}, \mu_{12}, \mu_{23}, K_{23}, \nu_{12})$, as defined, for example, in Christensen's (1979) book, by

$$a = \tfrac{1}{2}(K_{23} - \mu_{23}), \quad b = \mu_{23}, \quad c = \tfrac{1}{2}E_{11} + \tfrac{1}{2}\mu_{23} - 2\mu_{12} + \tfrac{1}{2}(1-2\nu_{12})^2 K_{23}, \tag{13}$$

$$d = 2(\mu_{12} - \mu_{23}), \quad e = \mu_{23} - (1-2\nu_{12})K_{23}, \tag{14}$$

where the x_1-axis is in the direction of transverse isotropy.

2.2.2 *Creep.* The constitutive equation for the steady-state creep strain rate is of the form

$$\dot{\boldsymbol{\varepsilon}}^{cr} = \mathbf{f}(\boldsymbol{\sigma}, s), \tag{15}$$

where $\mathbf{f}$ is a transversely isotropic function, and s is collection of material parameters such as the volume fraction of the fibers, the material constants that enter the constitutive equations of the matrix and the fibers, etc. Using the results of Liu (1982) together with the representation theorems for isotropic functions (Wang, 1970a,b; Smith, 1971), we can readily show that the most general form of the above constitutive equations is

$$\dot{\boldsymbol{\varepsilon}}^{cr} = a_1\mathbf{I} + 2a_2\boldsymbol{\sigma} + 3a_3\boldsymbol{\sigma}^2 + a_4\mathbf{a} + a_5(\boldsymbol{\sigma}\cdot\mathbf{a} + \mathbf{a}\cdot\boldsymbol{\sigma}) + a_6(\boldsymbol{\sigma}^2\cdot\mathbf{a} + \mathbf{a}\cdot\boldsymbol{\sigma}^2) \equiv \mathbf{f}(\boldsymbol{\sigma}, s), \tag{16}$$

where the a_is are functions of s, and the following five transversely isotropic invariants:

$$I_1 = \mathrm{tr}\,(\boldsymbol{\sigma}), \quad I_2 = \mathrm{tr}\,(\boldsymbol{\sigma}^2), \quad I_3 = \mathrm{tr}\,(\boldsymbol{\sigma}^3), \quad I_4 = \mathrm{tr}\,(\boldsymbol{\sigma}\cdot\mathbf{a}) = \mathbf{n}\cdot\boldsymbol{\sigma}\cdot\mathbf{n}, \quad I_5 = \mathrm{tr}\,(\boldsymbol{\sigma}^2\cdot\mathbf{a}) = \mathbf{n}\cdot\boldsymbol{\sigma}^2\cdot\mathbf{n}. \tag{17}$$

An alternative set of commonly used transversely isotropic invariants is given in Appendix A.

If the creep response of the material is incompressible, then the following equation must be satisfied for all values of $\boldsymbol{\sigma}$:

$$3a_1 + 2a_2 I_1 + 3a_3 I_2 + a_4 + 2a_5 I_4 + 2a_6 I_5 = 0. \tag{18}$$

We consider composite materials in which both the fibers and the matrix are isotropic with constitutive equations such that $\dot{\boldsymbol{\varepsilon}}^{cr}(-\boldsymbol{\sigma}) = -\dot{\boldsymbol{\varepsilon}}^{cr}(\boldsymbol{\sigma})$, and require that the constitutive equation of the composite, eqn (16), satisfies the condition $\dot{\boldsymbol{\varepsilon}}^{cr}(-\boldsymbol{\sigma}) = -\dot{\boldsymbol{\varepsilon}}^{cr}(\boldsymbol{\sigma})$ as well. Then, one can readily show that $\dot{\boldsymbol{\varepsilon}}^{cr}(\mathbf{0}) = \mathbf{0}$, and that the functions a_i are such that

$$a_i(-I_1, I_2, -I_3, -I_4, I_5) = -a_i(I_1, I_2, I_3, I_4, I_5) \quad \text{for} \quad i = 1, 3, 4, 6, \tag{19}$$

and

$$a_i(-I_1, I_2, -I_3, -I_4, I_5) = a_i(I_1, I_2, I_3, I_4, I_5) \quad \text{for} \quad i = 2, 5, \tag{20}$$

which imply that

$$a_1 = a_3 = a_4 = a_6 = 0 \quad \text{when} \quad I_1 = I_3 = I_4 = 0. \tag{21}$$

We assume next that the creep strain rate $\dot{\boldsymbol{\varepsilon}}^{cr}$ is derived from a creep potential $\Psi = \Psi(\boldsymbol{\sigma}, s)$. In view of the assumed transverse isotropy, Ψ must be of the form

$$\Psi = \Psi(I_1, I_2, I_3, I_4, I_5, s). \tag{22}$$

Using the chain rule, we can readily show that

$$\dot{\boldsymbol{\varepsilon}}^{cr} = \frac{\partial \Psi}{\partial \boldsymbol{\sigma}} = \sum_{i=1}^{5} \frac{\partial \Psi}{\partial I_i} \frac{\partial I_i}{\partial \boldsymbol{\sigma}} = a_1 \mathbf{I} + 2a_2 \boldsymbol{\sigma} + 3a_3 \boldsymbol{\sigma}^2 + a_4 \mathbf{a} + a_5 (\boldsymbol{\sigma} \cdot \mathbf{a} + \mathbf{a} \cdot \boldsymbol{\sigma}), \tag{23}$$

where now

$$a_i = \frac{\partial \Psi}{\partial I_i}. \tag{24}$$

Note that eqn (23) is a special case of the more general form, eqn (16), with $a_6 = 0$.

Consider now the case in which both the matrix material and fiber material creep according to the power-law equation, eqn (8). Since quadratic stress generators are absent in (8), we introduce the assumption that the corresponding creep equation for the composite does not involve quadratic stress generators either, i.e. $a_3 = \partial \Psi / \partial I_3 \equiv 0$. We emphasize, however, that this is meant to be only a reasonable *approximation*; in general, such quadratic generators may appear in eqn (23) even though they are absent in eqn (8).

Summarizing, we mention that the assumed constitutive equation for the creep strain rate of the fiber-reinforced material is

$$\dot{\boldsymbol{\varepsilon}}^{cr} = a_1 \mathbf{I} + 2a_2 \boldsymbol{\sigma} + a_4 \mathbf{a} + a_5 (\boldsymbol{\sigma} \cdot \mathbf{a} + \mathbf{a} \cdot \boldsymbol{\sigma}) \equiv \mathbf{f}(\boldsymbol{\sigma}, s). \tag{25}$$

3. IDENTIFICATION OF MATERIAL FUNCTIONS a_i

Let the coordinate axis x_3 be along the direction of the fibers, so that $\mathbf{n} = \mathbf{e}_3$, where $\mathbf{e}_3$ is the unit base vector along the x_3-axis. Then the constitutive equation, eqn (25), can be written as

$$\dot{\varepsilon}_{ij}^{cr} = a_1 \delta_{ij} + 2a_2 \sigma_{ij} + a_4 \delta_{i3} \delta_{j3} + a_5 (\sigma_{i3} \delta_{j3} + \delta_{i3} \sigma_{j3}), \tag{26}$$

or, equivalently

$$\dot{\varepsilon}_{11}^{cr} = a_1 + 2a_2 \sigma_{11}, \tag{27}$$

$$\dot{\varepsilon}_{22}^{cr} = a_1 + 2a_2 \sigma_{22}, \tag{28}$$

$$\dot{\varepsilon}_{33}^{cr} = a_1 + a_4 + 2(a_2 + a_5) \sigma_{33}, \tag{29}$$

$$\dot{\varepsilon}_{12}^{cr} = 2a_2 \sigma_{12}, \tag{30}$$

$$\dot{\varepsilon}_{23}^{cr} = (2a_2 + a_5) \sigma_{23}, \tag{31}$$

$$\dot{\varepsilon}_{31}^{cr} = (2a_2 + a_5) \sigma_{31}. \tag{32}$$

The relevant invariants I_i now take the form

$$I_1 = \mathrm{tr}(\boldsymbol{\sigma}), \quad I_2 = \mathrm{tr}(\boldsymbol{\sigma}^2), \quad I_4 = \sigma_{33}, \quad I_5 = \sigma_{31}^2 + \sigma_{32}^2 + \sigma_{33}^2. \tag{33}$$

Equations (27)–(32) show that:

- a_2 and a_5 relate to the response of the composite under shear, whereas a_1 and a_4 refer to longitudinal and transverse tension;

- if $a_5 = \partial W/\partial I_5 \equiv 0$, then the response of the material is identical under longitudinal (σ_{23}, σ_{31}) or transverse shear (σ_{12});
- in view of eqn (21), longitudinal shear loading (i.e. $\sigma_{13} \neq 0$ and/or $\sigma_{23} \neq 0$, other $\sigma_{ij} = 0$) causes longitudinal shear strain rates only, i.e. $\dot{\varepsilon}^{cr}_{11} = \dot{\varepsilon}^{cr}_{22} = \dot{\varepsilon}^{cr}_{33} = \dot{\varepsilon}^{cr}_{12} = 0$;
- in view of eqn (21), transverse shear loading (i.e. $\sigma_{12} \neq 0$, other $\sigma_{ij} = 0$) causes transverse shear strain rates only, i.e. $\dot{\varepsilon}^{cr}_{11} = \dot{\varepsilon}^{cr}_{22} = \dot{\varepsilon}^{cr}_{33} = \dot{\varepsilon}^{cr}_{13} = \dot{\varepsilon}^{cr}_{23} = 0$.

The last two conclusions are true even when the quadratic stress generator is included in the constitutive equation for $\dot{\varepsilon}^{cr}$, because the function a_3 vanishes under longitudinal or transverse shear, in view of eqn (21).

4. FINITE ELEMENT IMPLEMENTATION OF THE CONSTITUTIVE MODEL

In this section, we discuss the implementation of the general form of the constitutive model described in Section 2 in a finite element program. In a finite element environment, the solution of the creep problem is developed incrementally, and the constitutive equations are integrated at the element Gauss points. In a displacement-based finite element formulation, the solution is deformation driven. At a material point, the solution $(\boldsymbol{\sigma}_n, \boldsymbol{\varepsilon}_n)$ at time t_n as well as the strain $\boldsymbol{\varepsilon}_{n+1}$ at time $t_{n+1} = t_n + \Delta t$ is supposed to be known, and one has to determine the solution $\boldsymbol{\sigma}_{n+1}$.

4.1 *Numerical integration of the constitutive equations*

We start with the elasticity equation, eqn (10):

$$\boldsymbol{\sigma}_{n+1} = \mathbf{C} : \boldsymbol{\varepsilon}^e_{n+1} = \mathbf{C} : (\boldsymbol{\varepsilon}^e_n + \Delta\boldsymbol{\varepsilon} - \Delta\boldsymbol{\varepsilon}^{cr}) = \boldsymbol{\sigma}^e - \mathbf{C} : \Delta\boldsymbol{\varepsilon}^{cr}, \tag{34}$$

where $\Delta\boldsymbol{\varepsilon} = \boldsymbol{\varepsilon}_{n+1} - \boldsymbol{\varepsilon}_n$ and $\Delta\boldsymbol{\varepsilon}^{cr} = \boldsymbol{\varepsilon}^{cr}_{n+1} - \boldsymbol{\varepsilon}^{cr}_n$ are the total- and creep-strain increments, and $\boldsymbol{\sigma}^e = \boldsymbol{\sigma}_n + \mathbf{C} : \Delta\boldsymbol{\varepsilon}$ is the (known) elastic predictor.

The creep constitutive equation, eqn (25), is integrated by using a generalized trapezoidal method:

$$\Delta\boldsymbol{\varepsilon}^{cr} = [\alpha\mathbf{f}(\boldsymbol{\sigma}_{n+1}, s) + (1-\alpha)\mathbf{f}(\boldsymbol{\sigma}_n, s)]\Delta t \quad (0 \leqslant \alpha \leqslant 1). \tag{35}$$

When $\alpha = 0$, 1, or 1/2, the integration scheme reduces to the forward Euler, backward Euler, or the trapezoidal method, respectively.

Summarizing, we write

$$\mathbf{F}(\Delta\boldsymbol{\varepsilon}^{cr}) \equiv \Delta\boldsymbol{\varepsilon}^{cr} - [\alpha\mathbf{f}(\boldsymbol{\sigma}_{n+1}(\Delta\boldsymbol{\varepsilon}^{cr}), s) + (1-\alpha)\mathbf{f}(\boldsymbol{\sigma}_n, s)]\Delta t = 0, \tag{36}$$

where

$$\boldsymbol{\sigma}_{n+1}(\Delta\boldsymbol{\varepsilon}^{cr}) = \boldsymbol{\sigma}^e - \mathbf{C} : \Delta\boldsymbol{\varepsilon}^{cr}. \tag{37}$$

We choose $\Delta\boldsymbol{\varepsilon}^{cr}$ as the primary unknown and treat eqn (36) as the basic equation in which $\boldsymbol{\sigma}_{n+1}$ is defined by eqn (37). The solution is obtained by using Newton's method. The first estimate for $\Delta\boldsymbol{\varepsilon}^{cr}$ used to start the Newton loop is obtained by using a forward Euler scheme, i.e. $(\Delta\boldsymbol{\varepsilon}^{cr})_{\text{est}} = \mathbf{f}(\boldsymbol{\sigma}_n, t_n, s)\,\Delta t$. An alternative and more accurate estimate for $\Delta\boldsymbol{\varepsilon}^{cr}$ can be obtained by using the so-called "forward gradient" technique as described in the following. The function $\mathbf{f}(\boldsymbol{\sigma}_{n+1})$ is approximated by

$$\mathbf{f}(\boldsymbol{\sigma}_{n+1}) \simeq \mathbf{f}(\boldsymbol{\sigma}_n) + \left(\frac{\partial\mathbf{f}}{\partial\boldsymbol{\sigma}}\right)_n : \Delta\boldsymbol{\sigma} = \mathbf{f}(\boldsymbol{\sigma}_n) + \left(\frac{\partial\mathbf{f}}{\partial\boldsymbol{\sigma}}\right)_n : \mathbf{C} : (\Delta\boldsymbol{\varepsilon} - \Delta\boldsymbol{\varepsilon}^{cr}) \tag{38}$$

and substituted into eqn (36), which then yields the following estimate for $\Delta\boldsymbol{\varepsilon}^{cr}$:

$$(\Delta\boldsymbol{\varepsilon}^{cr})_{\text{est}} = \left[\mathbf{J}+\alpha\left(\frac{\partial \mathbf{f}}{\partial \boldsymbol{\sigma}}\right)_n : \mathbf{C}\Delta t\right]^{-1} : \left[\mathbf{f}(\boldsymbol{\sigma}_n)+\alpha\left(\frac{\partial \mathbf{f}}{\partial \boldsymbol{\sigma}}\right)_n : \mathbf{C} : \Delta\varepsilon\right]\Delta t. \tag{39}$$

The Jacobian associated with the Newton loop in eqn (36) is given by

$$\frac{\partial \mathbf{F}}{\partial \Delta\boldsymbol{\varepsilon}^{cr}} = \mathbf{J}-\alpha\Delta t\left(\frac{\partial \mathbf{f}}{\partial \boldsymbol{\sigma}}\right)_{n-1} : \frac{\partial \boldsymbol{\sigma}_{n-1}}{\partial \Delta\boldsymbol{\varepsilon}^{cr}} = \mathbf{J}+\alpha\Delta t\left(\frac{\partial \mathbf{f}}{\partial \boldsymbol{\sigma}}\right)_{n+1} : \mathbf{C}. \tag{40}$$

Once $\Delta\boldsymbol{\varepsilon}^{cr}$ is found, eqn (37) defines the stress $\boldsymbol{\sigma}_{n+1}$, and this completes the integration procedure.

In the following, we derive the general form of $\partial \mathbf{f}/\partial \boldsymbol{\sigma}$. Recalling the creep constitutive equation

$$\dot{\boldsymbol{\varepsilon}}^{cr} = \frac{\partial \Psi}{\partial \boldsymbol{\sigma}} = \sum_{i=1}^{5} \frac{\partial \Psi}{\partial I_i}\frac{\partial I_i}{\partial \boldsymbol{\sigma}} = \mathbf{f}(\boldsymbol{\sigma}), \tag{41}$$

we readily conclude that

$$\frac{\partial \mathbf{f}}{\partial \boldsymbol{\sigma}} = \frac{\partial^2 \Psi}{\partial \boldsymbol{\sigma}\,\partial \boldsymbol{\sigma}} = \sum_{i=1}^{5}\sum_{j=1}^{5} \frac{\partial^2 \Psi}{\partial I_i \partial I_j}\frac{\partial I_i}{\partial \boldsymbol{\sigma}}\frac{\partial I_j}{\partial \boldsymbol{\sigma}} + \sum_{i=1}^{5} \frac{\partial \Psi}{\partial I_i}\frac{\partial^2 I_i}{\partial \boldsymbol{\sigma}\,\partial \boldsymbol{\sigma}}, \tag{42}$$

where

$$\frac{\partial I_1}{\partial \boldsymbol{\sigma}} = \mathbf{I}, \quad \frac{\partial^2 I_1}{\partial \boldsymbol{\sigma}\,\partial \boldsymbol{\sigma}} = 0, \tag{43}$$

$$\frac{\partial I_2}{\partial \boldsymbol{\sigma}} = 2\boldsymbol{\sigma}, \quad \frac{\partial^2 I_2}{\partial \boldsymbol{\sigma}\,\partial \boldsymbol{\sigma}} = 2\mathbf{J}, \tag{44}$$

$$\frac{\partial I_3}{\partial \boldsymbol{\sigma}} = 3\boldsymbol{\sigma}^2, \quad \frac{\partial^2 I_3}{\partial \sigma_{ij}\,\partial \sigma_{kl}} = 3(\delta_{ik}\sigma_{lj}+\sigma_{ik}\delta_{lj}), \tag{45}$$

$$\frac{\partial I_4}{\partial \boldsymbol{\sigma}} = \mathbf{a}, \quad \frac{\partial^2 I_4}{\partial \boldsymbol{\sigma}\,\partial \boldsymbol{\sigma}} = 0, \tag{46}$$

$$\frac{\partial I_5}{\partial \boldsymbol{\sigma}} = \boldsymbol{\sigma}\cdot\mathbf{a}+\mathbf{a}\cdot\boldsymbol{\sigma}, \quad \frac{\partial^2 I_5}{\partial \sigma_{ij}\,\partial \sigma_{kl}} = a_{ik}\sigma_{lj}+\sigma_{ik}a_{lj}. \tag{47}$$

We conclude this section with a brief discussion of the appropriate time increment used in the integration procedure. Let $\sigma_{\max}$ be the maximum of the absolute values of the stress components (i.e. $\sigma_{\max} = \max|\sigma_{ij}|$) and define

$$\text{CETOL} = 0.1\frac{\sigma_{\max}}{E_{11}}, \tag{48}$$

where E_{11} is the elastic modulus defined in Section 2.2.1. The time increment Δt is chosen so that the maximum difference in the creep strain increment calculated from the creep strain rate based on the conditions at the beginning and at the end of the increment is always less than CETOL, i.e.

$$|f_{ij}(\boldsymbol{\sigma}_{n+1}) - f_{ij}(\boldsymbol{\sigma}_n)|\,\Delta t < \text{CETOL} \quad \text{for all } i, j. \tag{49}$$

4.2 *Linearization moduli*

In an implicit finite element code, the overall discretized equilibrium equations are written at the end of the increment, resulting in a set of non-linear equations for the nodal unknowns. If a full Newton scheme is used to solve the global non-linear equations, one needs to calculate the so-called "linearization moduli" $\mathscr{J}$, given by

$$\mathscr{J} = \frac{\partial \boldsymbol{\sigma}_{n+1}}{\partial \boldsymbol{\varepsilon}_{n-1}}. \tag{50}$$

For simplicity, we drop the subscript $(n+1)$ with the understanding that all quantities are evaluated at the end of the increment, unless otherwise indicated. Starting with the elasticity equation, eqn (34), we find

$$\partial\boldsymbol{\sigma} = \mathbf{C} : \partial\boldsymbol{\varepsilon} - \mathbf{C} : \partial\Delta\boldsymbol{\varepsilon}^{cr}. \tag{51}$$

The differential $\partial\Delta\boldsymbol{\varepsilon}^{cr}$ is evaluated from eqn (35) as follows:

$$\partial\Delta\boldsymbol{\varepsilon}^{cr} = \frac{\partial\Delta\boldsymbol{\varepsilon}^{cr}}{\partial\boldsymbol{\sigma}} : \partial\boldsymbol{\sigma} = \alpha\Delta t \frac{\partial \mathbf{f}}{\partial\boldsymbol{\sigma}} : \partial\boldsymbol{\sigma}. \tag{52}$$

Substituting the last equation into eqn (51) and solving for $\partial\boldsymbol{\sigma}/\partial\boldsymbol{\varepsilon}$, we find

$$\mathscr{J} = \frac{\partial\boldsymbol{\sigma}}{\partial\boldsymbol{\varepsilon}} = \left(\mathbf{J} + \alpha\Delta t \mathbf{C} : \frac{\partial \mathbf{f}}{\partial\boldsymbol{\sigma}}\right)^{-1} : \mathbf{C} = \left(\mathbf{C}^{-1} + \alpha\Delta t \frac{\partial \mathbf{f}}{\partial\boldsymbol{\sigma}}\right)^{-1}. \tag{53}$$

Note that $\partial f_{ij}/\partial\sigma_{kl}$ is symmetric with respect to the pair of indices (i,j) and (k,l). Hence, in view of eqn (53) and the usual symmetries of the elasticity tensor C, the Jacobian $\mathscr{J}_{ijkl}$ is also symmetric with respect to (i,j) and (k,l), which leads to a symmetric "stiffness matrix" in the finite element computations.

4.3 *The case of plane stress*

In this section, we consider the case in which the fibers are all parallel to the $x_3 = 0$ plane (i.e. $\mathbf{n} = n_1\mathbf{e}_1 + n_2\mathbf{e}_2$) and the applied loads are such that $\sigma_{33} = \sigma_{31} = \sigma_{32} = 0$. The stress and strain tensors are now of the form

$$\boldsymbol{\sigma} = \sigma_{\alpha\beta}\mathbf{e}_\alpha\mathbf{e}_\beta \quad \text{and} \quad \boldsymbol{\varepsilon} = \varepsilon_{\alpha\beta}\mathbf{e}_\alpha\mathbf{e}_\beta + \varepsilon_{33}\mathbf{e}_3\mathbf{e}_3, \tag{54}$$

where Greek subscripts range over the integers (1, 2).

In such problems, the strain increments $\Delta\varepsilon_{11}$, $\Delta\varepsilon_{22}$, and $\Delta\varepsilon_{12}$ are known, but the out-of-plane component of the strain increment $\Delta\varepsilon_{33}$ is not defined kinematically; some modifications to the method described in Section 4.1 are therefore needed.

The total- and creep-strain increments are written as

$$\Delta\boldsymbol{\varepsilon} = \Delta\varepsilon_{\alpha\beta}\mathbf{e}_\alpha\mathbf{e}_\beta + \Delta\varepsilon_{33}\mathbf{e}_3\mathbf{e}_3 \quad \text{and} \quad \Delta\boldsymbol{\varepsilon}^{cr} = \Delta\varepsilon^{cr}_{\alpha\beta}\mathbf{e}_\alpha\mathbf{e}_\beta + \Delta\varepsilon^{cr}_{33}\mathbf{e}_3\mathbf{e}_3. \tag{55}$$

The plane stress condition $\sigma_{33} = 0$ requires that

$$C_{33ij}(\Delta\varepsilon_{ij} - \Delta\varepsilon^{cr}_{ij}) = 0 \quad \textit{or} \quad \Delta\varepsilon_{33} = (C_{33ij}\Delta\varepsilon^{cr}_{ij} - C_{33\alpha\beta}\Delta\varepsilon_{\alpha\beta})/C_{3333}. \tag{56}$$

Summarizing, we write

$$\mathbf{F}(\Delta\boldsymbol{\varepsilon}^{cr}) \equiv \Delta\boldsymbol{\varepsilon}^{cr} - [\alpha\mathbf{f}(\boldsymbol{\sigma}(\Delta\boldsymbol{\varepsilon}^{cr}), s) + (1-\alpha)\mathbf{f}(\boldsymbol{\sigma}_n, s)]\Delta t = 0, \tag{57}$$

$$\sigma_{ij}(\Delta\boldsymbol{\varepsilon}^{cr}) = \hat{\sigma}^e_{ij} + C_{ij33}\Delta\varepsilon_{33}(\Delta\boldsymbol{\varepsilon}^{cr}) - C_{ijkl}\Delta\varepsilon^{cr}_{kl}, \tag{58}$$

$$\Delta\varepsilon_{33}(\Delta\boldsymbol{\varepsilon}^{cr}) = (C_{33ij}\Delta\varepsilon^{cr}_{ij} - C_{33\alpha\beta}\Delta\varepsilon_{\alpha\beta})/C_{3333}, \tag{59}$$

where

$$\hat{\sigma}^e_{ij} = (\boldsymbol{\sigma}_n)_{ij} + \mathrm{C}_{ij\alpha\beta}\Delta\varepsilon_{\alpha\beta}. \tag{60}$$

We choose $\Delta\boldsymbol{\varepsilon}^{cr}$ as the primary unknown and treat (57) as the basic equation in which $\boldsymbol{\sigma}(\Delta\boldsymbol{\varepsilon}^{cr})$ is defined by eqns (58)–(60). The solution is obtained by using Newton's method. The corresponding Jacobian is

$$\frac{\partial\mathbf{F}}{\partial\Delta\boldsymbol{\varepsilon}^{cr}} = \mathbf{J} - \alpha\Delta t\frac{\partial\mathbf{f}}{\partial\boldsymbol{\sigma}} : \frac{\partial\boldsymbol{\sigma}}{\partial\Delta\boldsymbol{\varepsilon}^{cr}} = \mathbf{J} + \alpha\Delta t\frac{\partial\mathbf{f}}{\partial\boldsymbol{\sigma}} : (\mathrm{C}-\mathrm{A}), \tag{61}$$

where

$$A_{ijlk} = C_{ij33}C_{33kl}/C_{3333}. \tag{62}$$

5. AN ANALYTICAL MODEL FOR CREEPING FIBER-REINFORCED MATERIALS

deBotton and Ponte Castañeda (1993) have recently presented a constitutive model for non-linear composite materials reinforced by continuous fibers. They developed their model in the context of infinitesimal non-linear elasticity, but their results can be used to describe *steady-state* creep as well. The derivation of the model is based on a variational principle that enables the expression of the effective energy functions of non-linear composites in terms of optimization problems.

For the special case of incompressible behavior in which the creep potential for both the matrix and the fibers is a function of the von Mises equivalent stress σ_e, their model can be summarized as follows. Let the creep potentials for the matrix and the fibers be of the form

$$\Psi^{(k)} = \Psi^{(k)}(\sigma_e), \quad k = 1, 2, \tag{63}$$

where $k = 1$ refers to the matrix and $k = 2$ to the fibers. If the matrix is the "weaker" material (i.e. $\Psi^{(1)}(\sigma_e) > \Psi^{(2)}(\sigma_e)$ for all σ_e), then the creep potential of the composite is estimated to be (deBotton and Ponte Castañeda, 1993)

$$\Psi(I_1, I_2, I_4) = \hat{\Psi}(\sigma_s^2, \sigma_d^2) = \min_{\omega,\eta}[c_1\Psi^{(1)}(\sigma_e^{(1)}) + c_2\Psi^{(2)}(\sigma_e^{(2)})], \tag{64}$$

where c_1 and c_2 are the volume fractions of the matrix and the fibers, respectively, $(c_1 + c_2 = 1)$, and

$$\sigma_e^{(1)}(\boldsymbol{\sigma}, \omega, \eta) = \{[(1+c_2\omega)^2 + c_2\omega^2]\sigma_s^2(\boldsymbol{\sigma}) + (1+c_2\eta)^2\sigma_d^2(\boldsymbol{\sigma})\}^{1/2}, \tag{65}$$

$$\sigma_e^{(2)}(\boldsymbol{\sigma}, \omega, \eta) = [(1-c_1\omega)^2\sigma_s^2(\boldsymbol{\sigma}) + (1-c_1\eta)^2\sigma_d^2(\boldsymbol{\sigma})]^{1/2}, \tag{66}$$

$$\sigma_s^2(\boldsymbol{\sigma}) = 3(\tau_n^2 + \tau_p^2) = \tfrac{1}{2}(3I_2 - I_1^2) - \tfrac{1}{4}(I_1 - 3I_4)^2, \tag{67}$$

$$\sigma_d^2(\boldsymbol{\sigma}) = (\sigma_n - \sigma_p)^2 = \tfrac{1}{4}(3I_4 - I_1)^2, \tag{68}$$

$$\sigma_n = \mathbf{n}\cdot\boldsymbol{\sigma}\cdot\mathbf{n}, \tag{69}$$

$$\sigma_p = \tfrac{1}{2}\boldsymbol{\sigma} : (\mathbf{I} - \mathbf{nn}). \tag{70}$$

The quantities σ_n, σ_p, τ_n, and τ_p are the alternative set of transversely isotropic invariants discussed in Appendix A.

Note that, in eqn (64), the creep potential Ψ is independent of I_5, which implies that the predicted response of the composite will be the same under longitudinal and transverse shear.

Let $\hat{\eta}$ and $\hat{\omega}$ be the values of η and ω that minimize the right-hand side of eqn (64) for a given stress state $\boldsymbol{\sigma}$, i.e.

$$\Psi = c_1 \Psi^{(1)}(\boldsymbol{\sigma}, \hat{\omega}, \hat{\eta}) + c_2 \Psi^{(2)}(\boldsymbol{\sigma}, \hat{\omega}, \hat{\eta}). \tag{71}$$

In general, $\hat{\eta}$ and $\hat{\omega}$ are functions of $\boldsymbol{\sigma}$, and the corresponding equation for the creep strain rate is

$$\dot{\boldsymbol{\varepsilon}}^{cr} = c_1 \frac{\partial \Psi^{(1)}}{\partial \boldsymbol{\sigma}} + c_2 \frac{\partial \Psi^{(2)}}{\partial \boldsymbol{\sigma}} + \left(c_1 \frac{\partial \Psi^{(1)}}{\partial \hat{\omega}} + c_2 \frac{\partial \Psi^{(2)}}{\partial \hat{\omega}} \right) \frac{\partial \hat{\omega}}{\partial \boldsymbol{\sigma}} + \left(c_1 \frac{\partial \Psi^{(1)}}{\partial \hat{\eta}} + c_2 \frac{\partial \Psi^{(2)}}{\partial \hat{\eta}} \right) \frac{\partial \hat{\eta}}{\partial \boldsymbol{\sigma}}. \tag{72}$$

However, in view of the minimization in eqn (64), each of the terms in parentheses on the right-hand side of the above equation vanishes identically. Therefore, in computing $\dot{\varepsilon}^{cr}$, one may regard $\hat{\omega}$ and $\hat{\eta}$ as constants (deBotton and Castañeda, 1993). The corresponding constitutive equation for the creep strain rate can be now written as

$$\dot{\varepsilon}_{ij}^{cr} = \left[c_1 \frac{\partial \Psi^{(1)}(\sigma_e^{(1)})}{\partial \sigma_{ij}} + c_2 \frac{\partial \Psi^{(2)}(\sigma_e^{(2)})}{\partial \sigma_{ij}} \right]_{\omega = \hat{\omega}, \eta = \hat{\eta}} \tag{73}$$

$$= c_1 \frac{\Psi^{(1)\prime}}{\sigma_e^{(1)}} \left\{ [(1 + c_2\hat{\omega})^2 + c_2\hat{\omega}^2]\sigma_s \frac{\partial \sigma_s}{\partial \sigma_{ij}} + (1 + c_2\hat{\eta})^2 \sigma_d \frac{\partial \sigma_d}{\partial \sigma_{ij}} \right\}$$

$$+ c_2 \frac{\Psi^{(2)\prime}}{\sigma_e^{(2)}} \left[(1 - c_1\hat{\omega})^2 \sigma_s \frac{\partial \sigma_s}{\partial \sigma_{ij}} + (1 - c_1\hat{\eta})^2 \sigma_d \frac{\partial \sigma_d}{\partial \sigma_{ij}} \right], \tag{74}$$

where

$$\Psi^{(k)\prime} = \left[\frac{d\Psi^{(k)}(\sigma_e)}{d\sigma_e} \right]_{\sigma_e = \sigma_e^{(k)}} \qquad k = 1, 2, \tag{75}$$

and

$$\sigma_s \frac{\partial \sigma_s}{\partial \sigma_{ij}} = \tfrac{3}{2}\sigma'_{ij} - \tfrac{1}{2}(\sigma_n - \sigma_p)(3n_i n_j - \delta_{ij}), \tag{76}$$

$$\sigma_d \frac{\partial \sigma_d}{\partial \sigma_{ij}} = \tfrac{1}{2}(\sigma_n - \sigma_p)(3n_i n_j - \delta_{ij}). \tag{77}$$

It should be noted that the above model is independent of the hydrostatic stress $p = \sigma_{kk}/3$ and that the predicted creep response is volume preserving, i.e. $\dot{\varepsilon}_{kk}^{cr} = 0$.

If the fibers are *rigid*, then one can formally set $\Psi^{(2)} = 0$. The minimization in eqn (64) then yields

$$\hat{\omega} = -\frac{1}{1+c_2} \quad \text{and} \quad \hat{\eta} = -\frac{1}{c_2}. \tag{78}$$

Then $\sigma_e^{(1)} = \sigma_s/\sqrt{1+c_2}$ and the estimated creep potential and the corresponding constitutive equations of the composite become

$$\Psi(I_1, I_2, I_4) = c_1 \Psi^{(1)}(\sigma_e^{(1)}), \tag{79}$$

$$\dot{\varepsilon}_{ij}^{cr} = \frac{c_1 \Psi^{(1)'}}{\sqrt{1+c_2}} \frac{\partial \sigma_s}{\partial \sigma_{ij}} = \frac{c_1}{2\sqrt{1+c_2}} \frac{\Psi^{(1)'}}{\sigma_s} [3\sigma'_{ij} - (\sigma_n - \sigma_p)(3n_i n_j - \delta_{ij})]. \tag{80}$$

Using the last equation, one can readily show that

$$\mathbf{n} \cdot \dot{\boldsymbol{\varepsilon}}^{cr} \cdot \mathbf{n} = 0, \tag{81}$$

i.e. the composite is inextensible in the direction of the rigid fibers. If $\mathbf{n} = \mathbf{e}_3$, then the constitutive equations (80) become

$$\dot{\varepsilon}_{11}^{cr} = -\dot{\varepsilon}_{22}^{cr} = \frac{A}{2}(\sigma'_{11} - \sigma'_{22}), \quad \dot{\varepsilon}_{33}^{cr} = 0, \quad \text{and} \quad \dot{\varepsilon}_{ij}^{cr} = A\sigma_{ij} \quad \text{for} \quad i \neq j, \tag{82}$$

where

$$A = \frac{3}{2} \frac{c_1}{\sqrt{1+c_2}} \frac{\Psi^{(1)'}}{\sigma_s}. \tag{83}$$

6. COMPARISON WITH RESULTS OF HOMOGENIZATION THEORY

The predictions of the constitutive model described in the previous section are compared here with the results of periodic homogenization theory (Sanchez-Palencia, 1980; Bakhvalov and Panasenko, 1989). The homogenization techniques were originally developed in the context of linear elasticity, but they have been extended to infinitesimal non-linear elasticity (Suquet, 1982; Jansson, 1992). The comparisons are carried out for non-linear elastic materials, for which the model of deBotton and Ponte Castañeda (1993) has been developed.

The non-linear composite is assumed to be *macroscopically homogeneous* and we seek to determine an *effective* constitutive equation of the form $\boldsymbol{\Sigma} = \mathbf{g}(\mathbf{E})$, where $\boldsymbol{\Sigma}$ and $\mathbf{E}$ are the macroscopic stress and strain respectively, and $\mathbf{g}$ is a tensor-valued constitutive function to be determined. The *macroscopic* field equations for a certain elasticity problem involving the composite then become

$$\frac{\partial \Sigma_{ji}}{\partial x_j} + b_i = 0, \tag{84}$$

$$\boldsymbol{\Sigma} = \mathbf{g}(\mathbf{E}), \tag{85}$$

$$E_{ij} = \frac{1}{2}\left(\frac{\partial u_i}{\partial x_j} + \frac{\partial u_j}{\partial x_i}\right), \tag{86}$$

where $\mathbf{u}$ is the displacement field, and $\mathbf{b} = \mathbf{b}(\mathbf{x})$ is the body force.

In the following, we summarize some of the results of homogenization theory as developed by Sanchez Palencia (1980) [see also Lene and Leguillon, 1982; Suquet, 1982, 1987; Lene, 1986; Jansson, 1992].

6.1 *Homogenization theory*

The composite is now modeled as an *inhomogeneous* continuum made of two different homogeneous non-linear elastic constituents. The microstructure is assumed to be *periodic*, i.e. the constituents of the composite are arranged in such a way that it can be constructed by the periodic repetition of self-similar elements. We define the "unit cell" as the smallest such repeatable element. The characteristic length l of the unit cell is assumed to be small compared with any characteristic dimension L of the body, i.e.

$$\delta = \frac{l}{L} \ll 1. \tag{87}$$

Let $\mathbf{x}$ denote the position vector with respect to a fixed global cartesian coordinate system. A local variable $\mathbf{y}$ is introduced for the unit cell by

$$\mathbf{y} = \frac{\mathbf{x}}{\delta} \quad \text{or} \quad \mathbf{x} = \delta\mathbf{y}, \tag{88}$$

so that a change of $O(1)$ in $\mathbf{y}$ corresponds to a change of $O(\delta)$ in $\mathbf{x}$. Note that the coordinate $\mathbf{x}$ is *constant* at the unit cell level, where positions are described in terms of $\mathbf{y}$.

In view of the periodicity of the microstructure, the constitutive equations at any point of the heterogeneous medium can be written as

$$\boldsymbol{\sigma} = \mathbf{f}\left(\boldsymbol{\varepsilon}, \frac{\mathbf{x}}{\delta}\right) = \mathbf{f}(\boldsymbol{\varepsilon}, \mathbf{y}), \tag{89}$$

$\mathbf{f}$ being a periodic function consistent with the periodicity of the microstructure, i.e. such that

$$\mathbf{f}\left(\boldsymbol{\varepsilon}, \frac{\mathbf{x}}{\delta} + l_i\mathbf{e}_i\right) = \mathbf{f}\left(\boldsymbol{\varepsilon}, \frac{\mathbf{x}}{\delta}\right), \quad i = 1, 2, 3 \quad \text{(no sum over } i\text{)} \tag{90}$$

where l_i is the characteristic length of the unit cell in the ith coordinate direction, and $\mathbf{e}_i$ is the unit vector in that direction. Functions of the type of eqn (90) will be referred to in the following as $\mathbf{Y}$-periodic.

Next, we search for an asymptotic expansion of the displacement field $\mathbf{u}$ as $\delta \to 0$. A two-scale expansion of the form (Sanchez Palencia, 1980)

$$\mathbf{u}(\mathbf{x}, \mathbf{y}) = \mathbf{u}^{(0)}(\mathbf{x}) + \delta\mathbf{u}^{(1)}(\mathbf{x}, \mathbf{y}) + \delta^2\mathbf{u}^{(2)}(\mathbf{x}, \mathbf{y}) + O(\delta^3) \tag{91}$$

is attempted, where the functions $\mathbf{u}^{(1)}$, $\mathbf{u}^{(2)}$, etc. are $\mathbf{Y}$-periodic. In the above equation, $\mathbf{u}^{(0)}(\mathbf{x})$ corresponds to the macroscopic deformation field $\mathbf{E}(\mathbf{x})$, whereas the subsequent $\mathbf{Y}$-periodic terms $\mathbf{u}^{(1)}$, $\mathbf{u}^{(2)}$, etc. are local perturbations due to the presence of the fibers in the continuum.

The corresponding strain expansion is

$$\boldsymbol{\varepsilon}(\mathbf{x}, \mathbf{y}) = [\mathbf{E}(\mathbf{x}) + \boldsymbol{\varepsilon}^{y(1)}(\mathbf{x}, \mathbf{y})] + \delta[\boldsymbol{\varepsilon}^{x(1)}(\mathbf{x}, \mathbf{y}) + \boldsymbol{\varepsilon}^{y(2)}(\mathbf{x}, \mathbf{y})] + O(\delta^2) \tag{92}$$

$$\equiv \boldsymbol{\varepsilon}^{(0)}(\mathbf{x}, \mathbf{y}) + \delta\boldsymbol{\varepsilon}^{(1)}(\mathbf{x}, \mathbf{y}) + O(\delta^2), \tag{93}$$

where

$$\varepsilon_{ij}^{x(k)} = \frac{1}{2}\left(\frac{\partial u_i^{(k)}}{\partial x_j} + \frac{\partial u_j^{(k)}}{\partial x_i}\right) \quad \text{and} \quad \varepsilon_{ij}^{y(k)} = \frac{1}{2}\left(\frac{\partial u_i^{(k)}}{\partial y_j} + \frac{\partial u_j^{(k)}}{\partial y_i}\right). \tag{94}$$

Note that $\boldsymbol{\varepsilon}^{x(0)}(\mathbf{x}) = \mathbf{E}(\mathbf{x})$. The stress field can be written as

$$\boldsymbol{\sigma}(\mathbf{x},\mathbf{y}) = \mathbf{f}(\boldsymbol{\varepsilon}^{(0)},\mathbf{y}) + \delta\mathbf{c}(\boldsymbol{\varepsilon}^{(0)},\mathbf{y}):\boldsymbol{\varepsilon}^{(1)} + O(\delta^2) \equiv \boldsymbol{\sigma}^{(0)}(\mathbf{x},\mathbf{y}) + \delta\boldsymbol{\sigma}^{(1)}(\mathbf{x},\mathbf{y}) + O(\delta^2), \tag{95}$$

where

$$\mathbf{c}(\boldsymbol{\varepsilon}^{(0)},\mathbf{y}) = \left[\frac{\partial \mathbf{f}(\boldsymbol{\varepsilon},\mathbf{y})}{\partial \boldsymbol{\varepsilon}}\right]_{\boldsymbol{\varepsilon}=\boldsymbol{\varepsilon}^{(0)}}. \tag{96}$$

The equilibrium equations become

$$\frac{1}{\delta}\frac{\partial \sigma_{ji}^{(0)}}{\partial y_j} + \left(\frac{\partial \sigma_{ji}^{(0)}}{\partial x_j} + \frac{\partial \sigma_{ji}^{(1)}}{\partial y_j} + b_i\right) + O(\delta) = 0. \tag{97}$$

In view of the **Y**-periodicity of $\mathbf{u}^{(1)}$ and **f**, the fields $\boldsymbol{\varepsilon}^{(0)}$, $\boldsymbol{\varepsilon}^{(1)}$, $\boldsymbol{\sigma}^{(0)}$, and $\boldsymbol{\sigma}^{(1)}$ are **Y**-periodic as well. Moreover, since the outward unit normal **N** to the boundary ∂Y of the unit cell takes opposite values on opposite sides of ∂Y, the traction vector $\mathbf{t}^{(0)} = \mathbf{N}\cdot\boldsymbol{\sigma}^{(0)}$ is **Y**-anti-periodic.

Collecting terms having like powers of δ, we obtain the following hierarchy of problems.

6.1.1 *Leading-order problem* (*the unit cell problem*). We can recast the leading-order terms of the above equations in the following form:

$$\hat{\mathbf{u}}(\mathbf{y}) \equiv \mathbf{E}(\mathbf{x})\cdot\mathbf{y} + \mathbf{u}^{(1)}(\mathbf{x},\mathbf{y}), \tag{98}$$

$$\hat{\varepsilon}_{ij}(\mathbf{y}) \equiv \varepsilon_{ij}^{(0)}(\mathbf{x},\mathbf{y}) = \frac{1}{2}\left(\frac{\partial \hat{u}_i}{\partial y_j} + \frac{\partial \hat{u}_j}{\partial y_i}\right), \tag{99}$$

$$\hat{\boldsymbol{\sigma}}(\mathbf{y}) \equiv \boldsymbol{\sigma}^{(0)}(\mathbf{x},\mathbf{y}) = \mathbf{f}(\hat{\boldsymbol{\varepsilon}},\mathbf{y}), \tag{100}$$

$$\frac{\partial \hat{\sigma}_{ji}}{\partial y_j} = 0, \tag{101}$$

with

$$\mathbf{u}^{(1)} \quad \mathbf{Y}\text{-periodic}, \qquad \hat{\mathbf{t}} = \mathbf{N}\cdot\hat{\boldsymbol{\sigma}} \quad \mathbf{Y}\text{-anti-periodic}, \tag{102}$$

where $\hat{\mathbf{u}}(\mathbf{y})$, $\hat{\boldsymbol{\varepsilon}}(\mathbf{y})$, and $\hat{\boldsymbol{\sigma}}(\mathbf{y})$ are the displacements, strains, and stresses of the unit cell, respectively. Recall that **x** is constant at the unit cell level; hence, the macroscopic strain field **E**(**x**) is also constant in eqn (98) and can be viewed as the macroscopic "applied load" to the unit cell. The field equations (98)–(101) over the unit cell together with the conditions (102) define a well-posed boundary value problem that can be solved for $(\hat{\mathbf{u}},\hat{\boldsymbol{\varepsilon}},\hat{\boldsymbol{\sigma}})$ or, equivalently, for $(\mathbf{u}^{(1)},\boldsymbol{\varepsilon}^{(0)},\boldsymbol{\sigma}^{(0)})$ [e.g. see Suquet (1987)]. One can readily show that, if the constitutive function **f** in eqn (89) is convex, then the unit cell problem has a unique solution.

For any function $\phi(\mathbf{x},\mathbf{y})$, we define

$$\langle\phi\rangle = \frac{1}{|Y|}\int_Y \phi(\mathbf{x},\mathbf{y})\,dV_y, \tag{103}$$

where Y denotes the unit cell. Using eqns (99) and (100) and taking into account the **Y**-periodicity of $\mathbf{u}^{(1)}$, we find

$$\langle \hat{\boldsymbol{\varepsilon}} \rangle = \langle \boldsymbol{\varepsilon}^{(0)} \rangle = \boldsymbol{\varepsilon}^{x(0)} = \mathbf{E} \quad \text{and} \quad \langle \hat{\boldsymbol{\sigma}} \rangle = \langle \boldsymbol{\sigma}^{(0)} \rangle. \tag{104}$$

The solution of the unit cell problem can be used to determine the functional relationship between $\langle \hat{\boldsymbol{\sigma}} \rangle$ and $\langle \hat{\varepsilon} \rangle$, i.e. to find a tensor-valued function $\mathbf{h}$ such that

$$\langle \hat{\boldsymbol{\sigma}} \rangle = \mathbf{h}(\langle \hat{\varepsilon} \rangle). \tag{105}$$

Note that, in view of eqn (104), the last equation can be also written as

$$\langle \boldsymbol{\sigma}^{(0)} \rangle = \mathbf{h}(\langle \boldsymbol{\varepsilon}^{(0)} \rangle). \tag{106}$$

We conclude this section by stating the well-known result

$$\langle \hat{\sigma}_{ij} \rangle = \frac{1}{2Y} \int_{\partial Y} (\hat{t}_i y_j + \hat{t}_j y_i) \, \mathrm{d}S_y. \tag{107}$$

6.1.2 *Second-order equations.* The equilibrium equation yields, to second order,

$$\frac{\partial \sigma_{ji}^{(0)}(\mathbf{x}, \mathbf{y})}{\partial x_j} + \frac{\partial \sigma_{ji}^{(1)}(\mathbf{x}, \mathbf{y})}{\partial y_j} + b_i(\mathbf{x}) = 0. \tag{108}$$

Taking the Y-average of the above equation and using the fact that $\boldsymbol{\sigma}^{(1)}$ is Y-periodic, we find

$$\frac{\partial \langle \sigma_{ji}^{(0)} \rangle}{\partial x_j} + b_i = 0. \tag{109}$$

We summarize our findings by restating eqns (109), (106), (104a) and (94a) as follows

$$\frac{\partial \langle \sigma_{ji}^{(0)} \rangle}{\partial x_j} + b_i = 0, \tag{110}$$

$$\langle \boldsymbol{\sigma}^{(0)} \rangle = \mathbf{h}(\langle \boldsymbol{\varepsilon}^{(0)} \rangle), \tag{111}$$

$$\langle \varepsilon_{ij}^{(0)} \rangle = \frac{1}{2} \left(\frac{\partial u_i^{(0)}}{\partial x_j} + \frac{\partial u_j^{(0)}}{\partial x_i} \right). \tag{112}$$

Equations (110)–(112) define the *homogenized problem* for $\mathbf{u}^{(0)}(\mathbf{x})$. Comparing eqns (110)–(112) with the macroscopic field equations (84)–(86), we conclude that the function $\mathbf{h}$, determined from the solution of the unit cell problem, provides the leading-order *homogenized* constitutive equation for the composite.

In the following, we use the finite element method to obtain numerical solutions of the unit cell problem for various types of loading. The solutions are then used to calculate numerically the function $\mathbf{h}$, which is the leading-order constitutive function of the homogenized composite.

6.2 *Numerical solution of the unit cell problem*

We consider a composite material made of a non-linear elastic matrix reinforced by continuous aligned fibers, which are assumed to be non-linear elastic as well. The constitutive equations for the matrix and the fibers are of the form

$$\varepsilon = \frac{\partial \Psi^{(k)}}{\partial \sigma} = \tfrac{3}{2}\varepsilon_{0k}\left(\frac{\sigma_e}{\sigma_{0k}}\right)^{n_k-1}\frac{\sigma'}{\sigma_{0k}}, \quad \Psi^{(k)}(\sigma_e) = \frac{\sigma_{0k}\varepsilon_{0k}}{n_k+1}\left(\frac{\sigma_e}{\sigma_{0k}}\right)^{n_k+1}, \quad k = 1,2. \tag{113}$$

The distribution of the fibers is assumed to be periodic, with the fibers arranged in a hexagonal array. The linear and quadratic stress invariants of the hexagonal arrangement are the same as those of a transversely isotropic system; a hexagonal array of fibers can therefore be used to study *linear* transversely isotropic elastic materials, since the elastic potential is a function of the linear and quadratic stress invariants only (Green and Adkins, 1960; Jansson, 1992). In the general case, however, where terms of higher degree are involved, the hexagonal system will provide only an *approximation* for a *non-linear* transversely isotropic material; the approximation will be less accurate with increasing non-linearity.

The fibers are assumed to be aligned with the y_3 coordinate direction, and the unit cell is infinitely long in that direction. Figure 1 shows the cross-section of the unit cell on the y_1–y_2 plane.

In the first set of calculations, the macroscopic applied loads are taken to coincide with the principal material directions. In particular, the following four types of loading are considered:

1. longitudinal tension: $\Sigma_{33} \neq 0$, all other $\Sigma_{ij} = 0$,
2. transverse tension: $\Sigma_{11} \neq 0$, all other $\Sigma_{ij} = 0$,
3. transverse shear: $\Sigma_{12} = \Sigma_{21} \neq 0$, all other $\Sigma_{ij} = 0$,
4. longitudinal shear: $\Sigma_{31} = \Sigma_{13} \neq 0$, all other $\Sigma_{ij} = 0$.

The unit cell problem is solved by using the ABAQUS general purpose finite element program (Hibbitt, 1984). The calculations are carried out for $n_1 = 10, n_2 = 3, \sigma_{01} = \sigma_{02} = \sigma_0$, and $\varepsilon_{01} = \varepsilon_{02} = \varepsilon_0$; note that $\Psi^{(1)}(\sigma_e) > \Psi^{(2)}(\sigma_e)$ for $\sigma_e/\sigma_0 > (11/4)^{1/7} = 1.16$. The "deformation plasticity" model in ABAQUS has an additional "linear-elastic" term on the right-hand side of eqn (113a); the elastic moduli used in the finite element computations are four orders of magnitude larger than σ_0, so that the contribution of the additional elastic terms

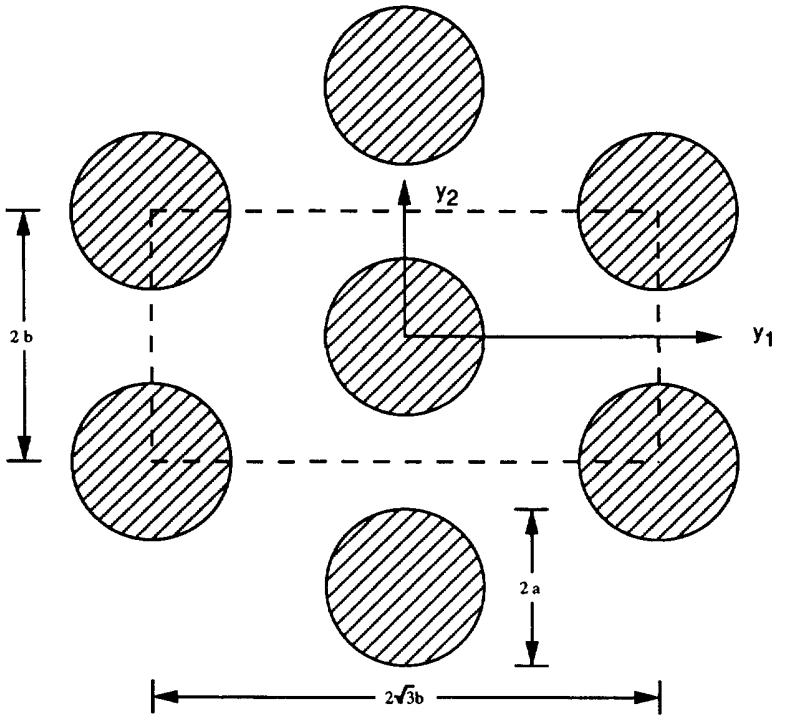

Fig. 1. Hexagonal array of fibers and the corresponding unit cell.

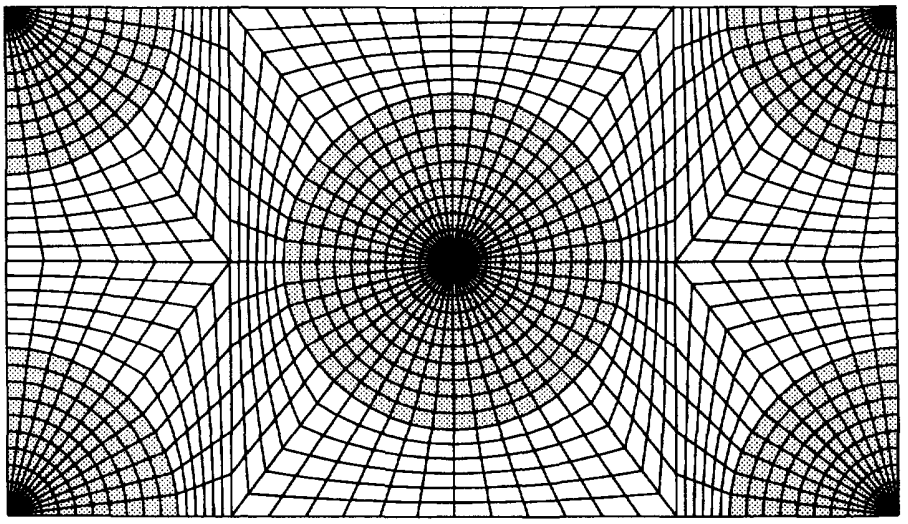

Fig. 2. Finite element mesh.

becomes negligible. The volume fraction of the fibers is 39.5%, i.e. $c_2 = 0.395$, $c_1 = 0.605$. Figure 2 shows the finite element mesh used in the problems that do not involve longitudinal shear (i.e. $\Sigma_{13} = 0$); the dark and white regions in Fig. 2 represent the fibers and the matrix, respectively. The layout shown in Fig. 2 is repeated in the third direction to produce the layer of three-dimensional elements used for the solution of the problems that involve longitudinal shear. The type of elements and the exact boundary conditions used in the calculation are discussed in Appendix B.

Figure 3 shows the calculated macroscopic stress–strain curves. In Fig. 3, the dotted line is the prediction of the model of deBotton and Ponte Castañeda, whereas the solid line indicates the results of the finite element calculations. Figure 3(a) shows the calculated longitudinal stress–strain curve. The predictions of the analytical model agree well with the solution of the unit cell problem. Figure 3(b) shows the calculated transverse stress–strain curve. At a transverse strain $E_{11} = 10\varepsilon_0$, there is less than 2% difference between the prediction of the analytical model and the finite element solution. Figure 3(c) shows the transverse shear stress–strain response. At a transverse shear strain $2E_{12} = 10\gamma_0$ ($\gamma_0 = \sqrt{3}\,\varepsilon_0$), there is a less than 8% difference between the prediction of the analytical model and the unit cell solution. The finite element solution of the problem of longitudinal shear produces a shear stress–strain curve identical to that shown in Fig. 3(c) for the transverse shear. This is consistent with the structure of the analytical model, which also predicts an identical response to longitudinal and transverse shear.

Figure 4 shows the calculated macroscopic stress–strain response when equal amounts of normal and shear stresses are applied simultaneously; Figs 4(a) and 4(b) correspond to combined transverse tension and shear and Figs 4(c) and 4(d) show that the corresponding results agree well with the predictions of the analytical model. Note that, for any given point (E_{11}, Σ_{11}) on Fig. 4(a), the corresponding point on Fig. 4(b) is that for which $\Sigma_{12} = \Sigma_{11}$. A similar comment applies to Figs 4(c) and 4(d).

Figures 3 and 4 show that, at a given strain level, the stress predicted by the analytical model is always higher than that of the finite element solution. This is consistent with the fact that the complementary elastic energy function Ψ developed by deBotton and Ponte Castañeda is an upper bound to the actual complementary energy of the composite. It should also be noted that the model of deBotton and Ponte Castañeda is developed for a transversely isotropic composite with a *random* distribution of fibers, whereas the unit cell calculations refer to a composite with a given *periodic* microstructure (hexagonal array).

7. AN EXAMPLE: A PLATE WITH A HOLE

The model of deBotton and Ponte Castañeda is implemented in the ABAQUS general purpose finite element program. This code provides a general interface so that a specific

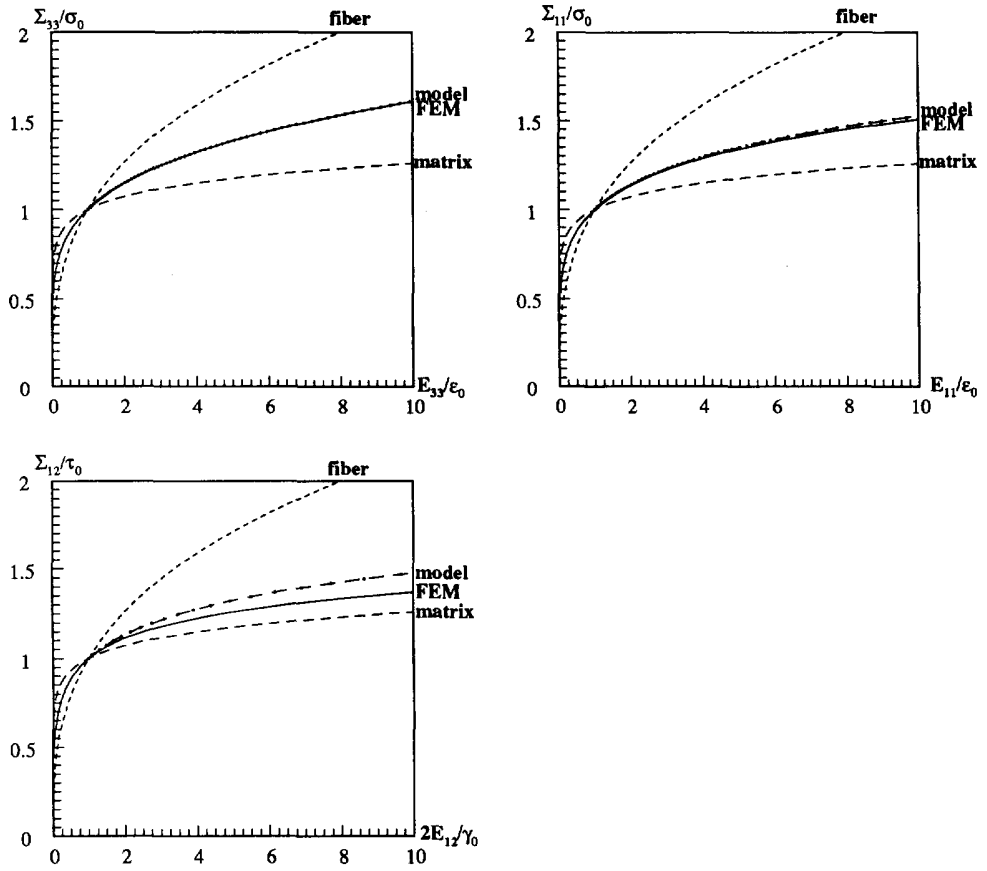

Fig. 3. (a) Longitudinal stress–curve. (b) Transverse stress–strain curve. (c) Stress–strain curve for transverse shear ($\tau_0 = \sigma_0/\sqrt{3}$, $\gamma_0 = \sqrt{3}\varepsilon_0$).

constitutive model can be introduced as a "user subroutine." The constitutive equations are integrated by using the method presented in Section 4 with $\alpha = 1/2$ (trapezoidal method).

Figure 5 shows a schematic representation of a plate with a hole; the plate is reinforced by continuous aligned fibers as shown in the figure, and the ratio $w/2a$ equals 6. Elasticity and creep are assumed to be the only possible mechanisms of deformation. The diameter of a typical fiber is assumed to be small compared with the size of the hole and the thickness of the plate, so that the continuum model described in Section 5 can be used in the calculations. As a model material, we consider a γ-TiAl matrix reinforced by polycrystalline Al_2O_3 continuous fibers. The fiber volume fraction is assumed to be 20%, i.e. $c_2 = 0.20$. Typical values of the elastic constants are $E = 200$ GPa and $\nu = 0.3$ for γ-TiAl, and $E = 385$ GPa and $\nu = 0.33$ for Al_2O_3, where E and ν are Young's modulus and Poisson's ratio, respectively. Using the estimation procedure described by Christensen (1979), we find the following values for the elastic constants of the composite: $E_{11} = 235$ GPa, $\mu_{12} = 85$ GPa, $\mu_{23} = 85$ GPa, $K_{23} = 220$ GPa, and $\nu_{12} = 0.31$. The matrix and the fibers are assumed to creep according to a power-law equation of the form

$$\dot{\boldsymbol{\varepsilon}}^{cr} = \frac{\partial \Psi^{(k)}}{\partial \boldsymbol{\sigma}} = \tfrac{3}{2}\dot{\varepsilon}_{0k}\left(\frac{\sigma_e}{\sigma_{0k}}\right)^{n_k-1}\frac{\boldsymbol{\sigma}'}{\sigma_{0k}}, \quad \Psi^{(k)}(\sigma_e) = \frac{\sigma_{0k}\dot{\varepsilon}_{0k}}{n_k+1}\left(\frac{\sigma_e}{\sigma_{0k}}\right)^{n_k+1}, \quad k = 1,2. \tag{114}$$

The model of deBotton and Ponte Castañeda is used to describe the creep behavior of the composite. The following creep constants are used in the computations: $n_1 = 2.6$ and $\dot{\varepsilon}_{01}/\sigma_{01}^{n_1} = 1.304 \times 10^{-9}$ MPa$^{-n_1}\cdot s^{-1}$ for the matrix, and $n_2 = 1$ and $\dot{\varepsilon}_{02}/\sigma_{02}^{n_2} = 10^{-9}$ MPa$^{-n_2}\cdot s^{-1}$ for the fibers.

Plane stress conditions are assumed, and two types of loading are considered, in which a constant tensile stress of 70 MPa is applied (a) in the direction of the fibers, and (b) in

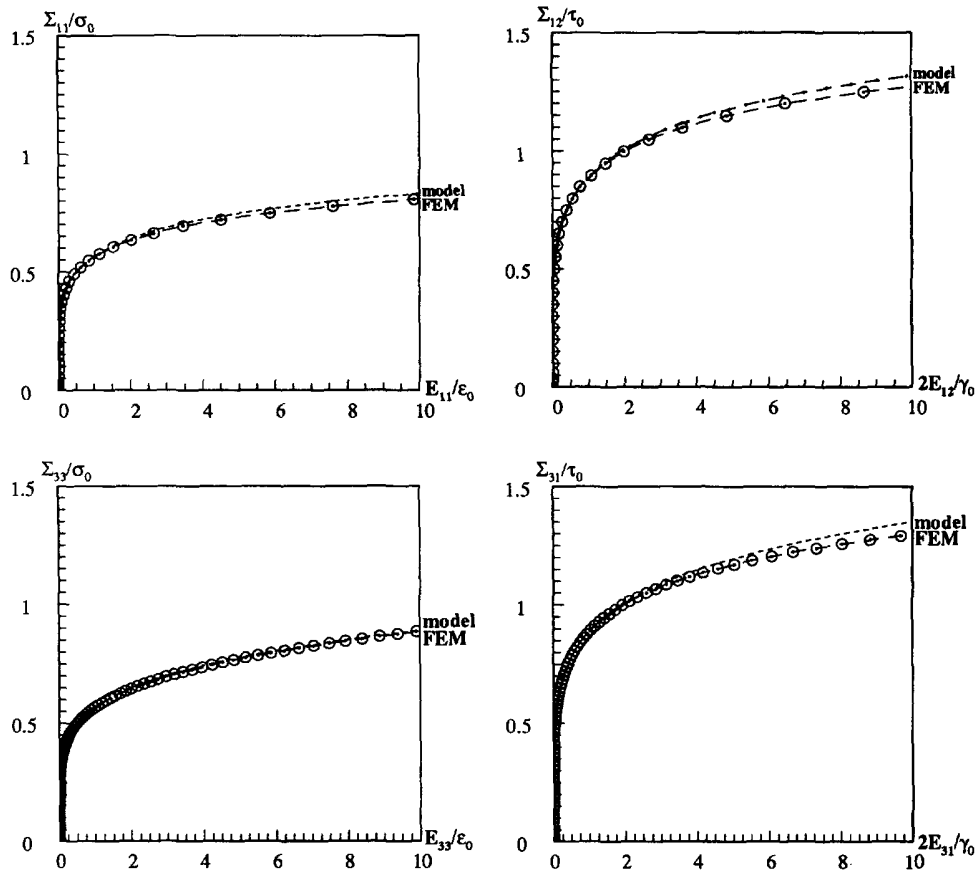

Fig. 4. (a), (b) Stress–strain curves for the combined transverse tension and shear with $\Sigma_{11} = \Sigma_{12} = \Sigma_{21}$. (c), (d) Stress–strain curves for the combined longitudinal tension and shear with $\Sigma_{33} = \Sigma_{13} = \Sigma_{31}$.

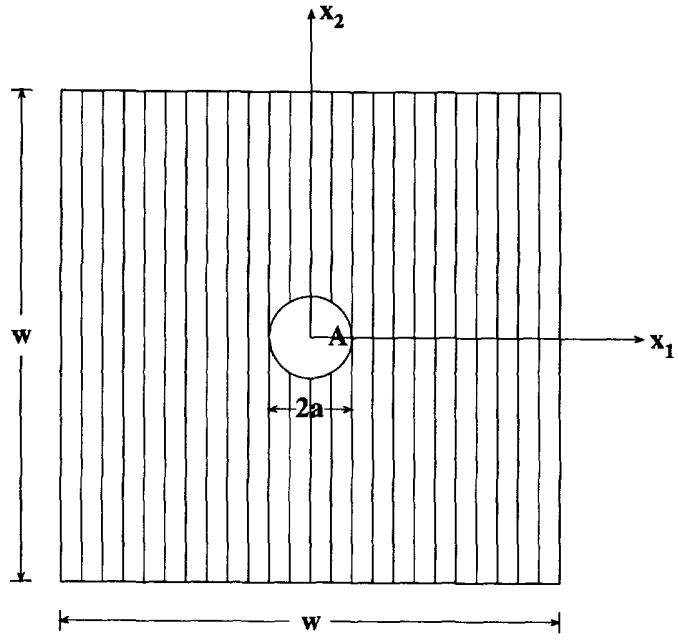

Fig. 5. Schematic representation of a plate with a hole. The fibers are in the x_2 coordinate direction.

the transverse direction. In both cases, the load is applied suddenly to the plate at the time $t = 0$. The instantaneous response of the material is elastic, and the elastic stress distribution provides the initial condition for the creep problem.

Four-node isoparametric elements with 2×2 Gauss integrations are used in the calculations. The analysis is carried out incrementally, and the maximum size of the time increment is controlled by the formula in eqn (49). At every element integration point, the values of $\hat{\omega}$ and $\hat{\eta}$ that minimize the right-hand side of eqn (64) are found by using the values of the stress tensor $\boldsymbol{\sigma}_n$ at the beginning of each increment.

Figures 6–9 show contour plots of several transversely isotropic invariants of the creep strain $\boldsymbol{\varepsilon}^{cr}$ at a time $t = 1$ h for both cases analyzed. The invariants plotted in these figures are (deBotton and Ponte Castañeda, 1993):

$$\varepsilon_p^{cr} = \tfrac{1}{2}\boldsymbol{\varepsilon}^{cr} : \boldsymbol{\beta} = \tfrac{1}{2}(\varepsilon_{11}^{cr} + \varepsilon_{33}^{cr}), \tag{115}$$

$$\varepsilon_n^{cr} = \boldsymbol{\varepsilon}^{cr} : \mathbf{a} = \varepsilon_{22}^{cr}, \tag{116}$$

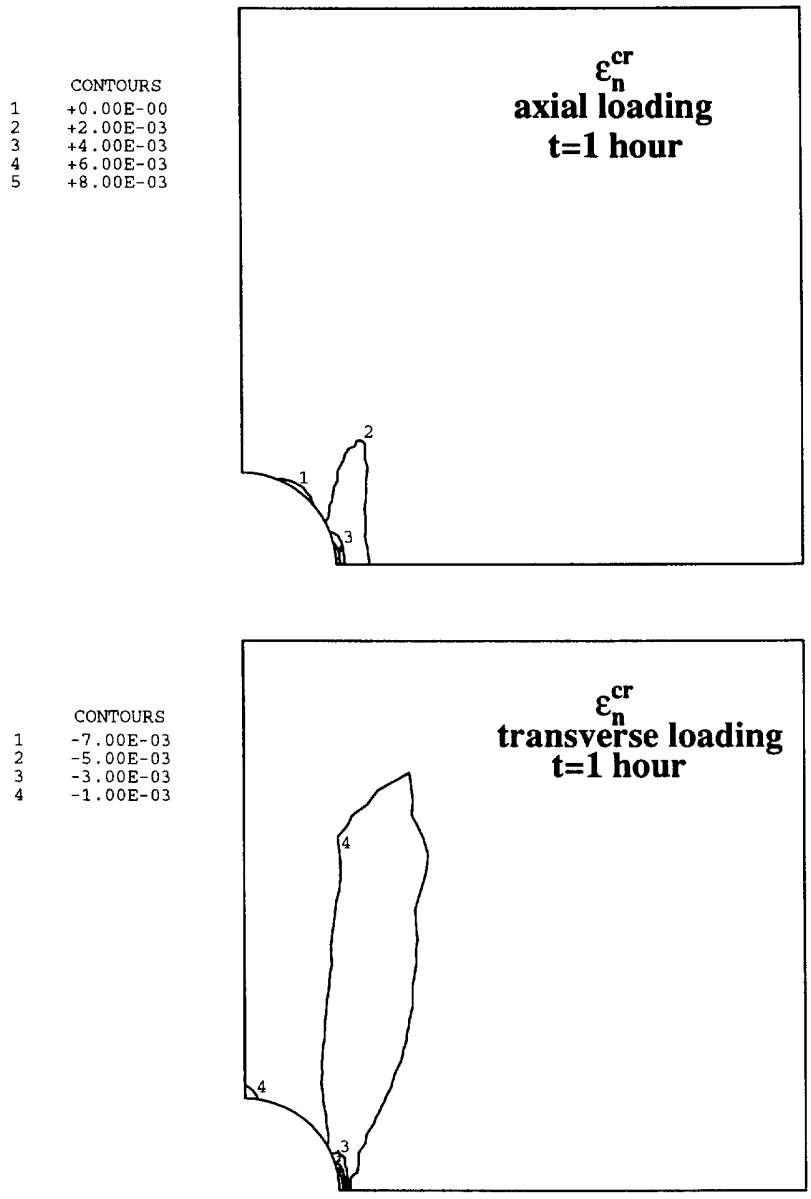

Fig. 6. Contours of creep strain invariant ε_n.

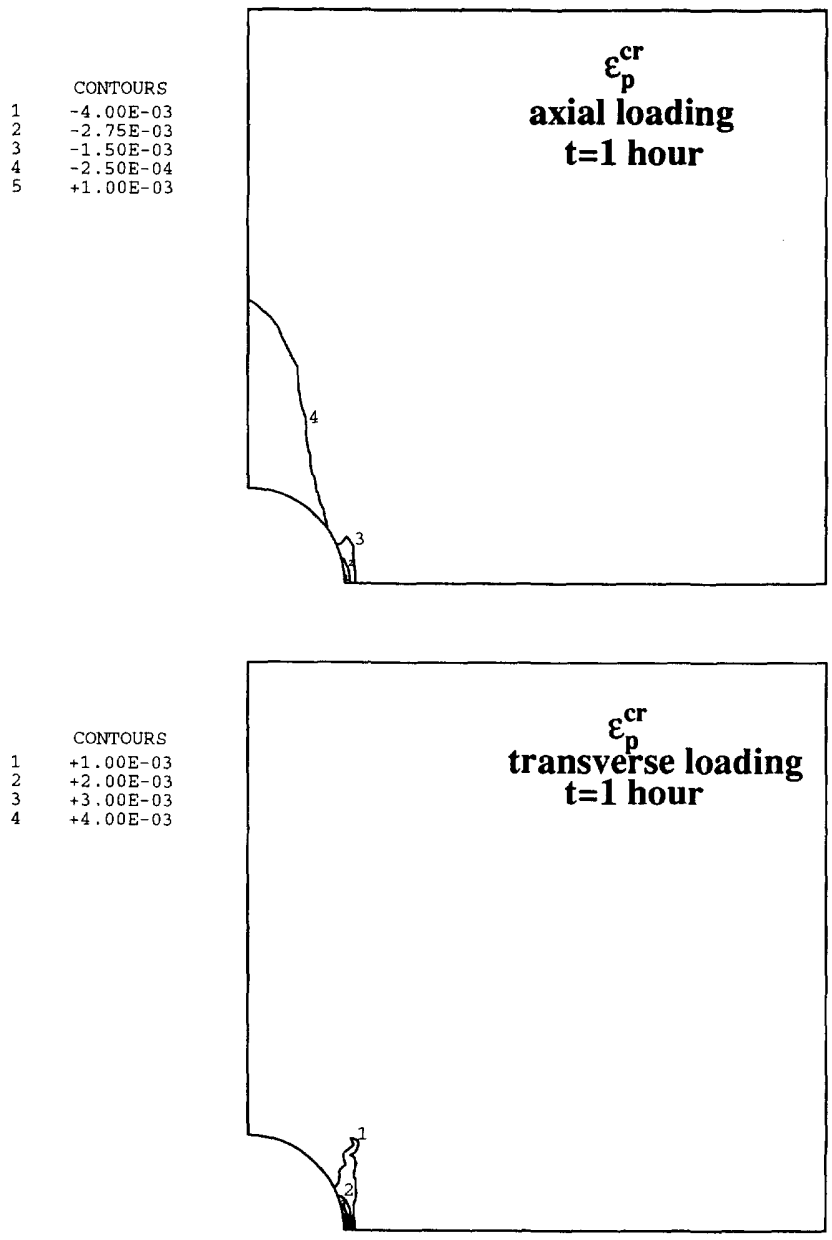

Fig. 7. Contours of creep strain invariant ε_p.

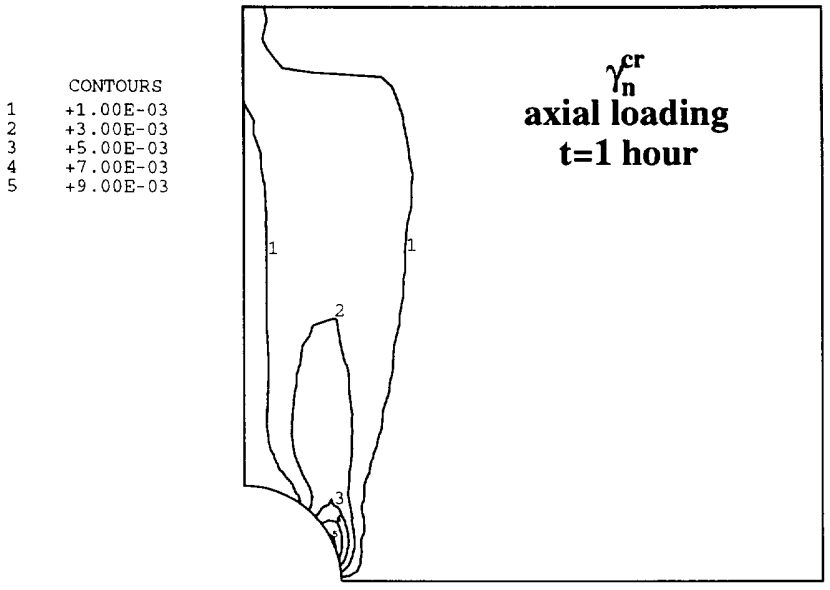

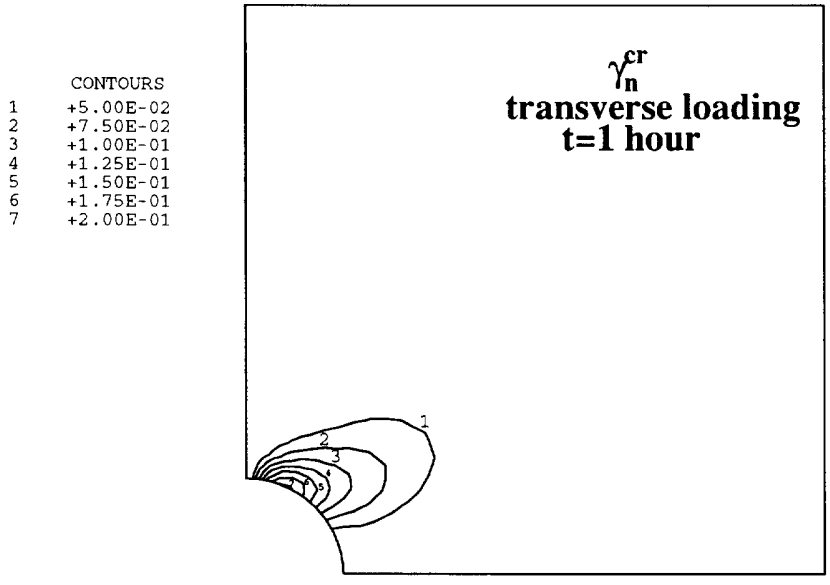

Fig. 8. Contours of creep strain invariant γ_n.

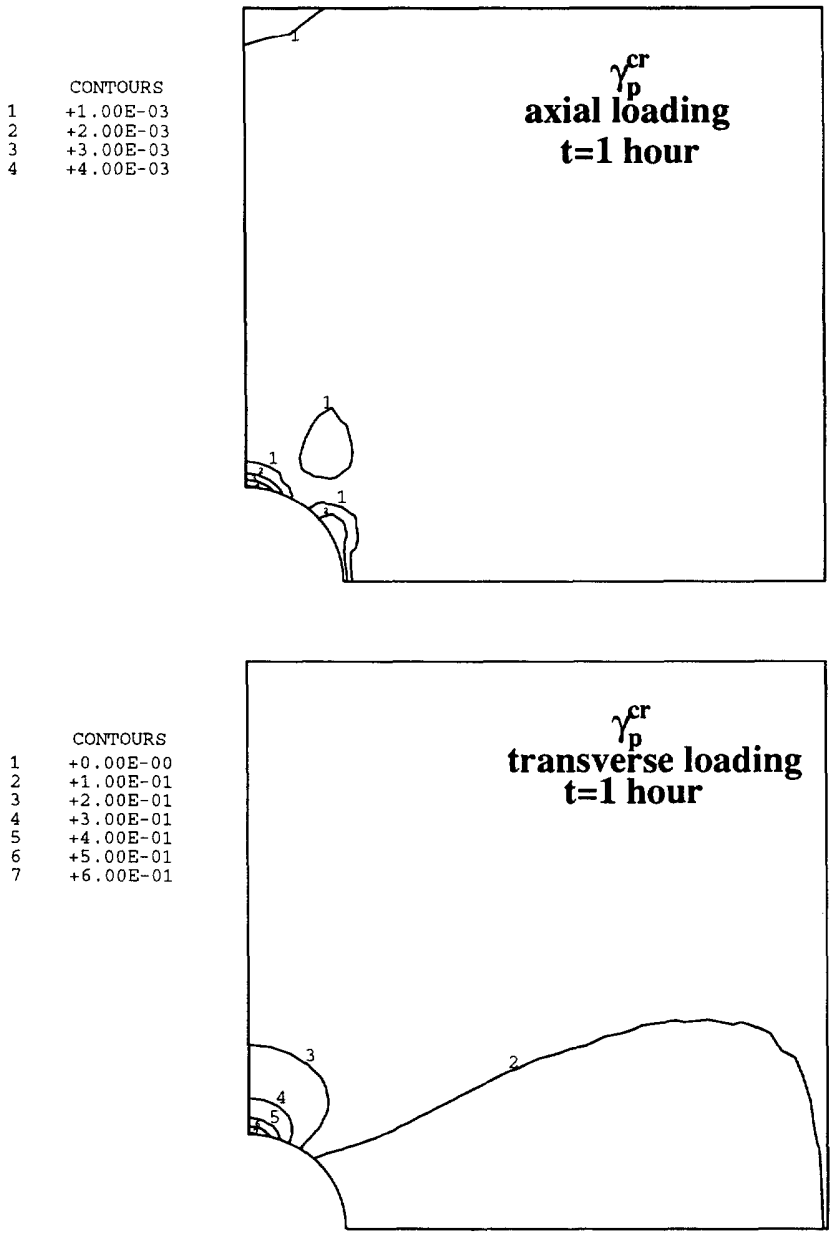

Fig. 9. Contours of creep strain invariant γ_p.

$$(\gamma_p^{cr})^2 = \tfrac{1}{2}(\boldsymbol{\varepsilon}^{cr}\cdot\boldsymbol{\beta}):(\boldsymbol{\varepsilon}^{cr}\cdot\boldsymbol{\beta}) - \tfrac{1}{4}(\boldsymbol{\varepsilon}^{cr}:\boldsymbol{\beta})^2 = (\varepsilon_{13}^{cr})^2 + \tfrac{1}{4}(\varepsilon_{11}^{cr} - \varepsilon_{33}^{cr})^2, \tag{117}$$

$$(\gamma_n^{cr})^2 = (\boldsymbol{\varepsilon}^{cr})^2 : \mathbf{a} - (\boldsymbol{\varepsilon}^{cr}:\mathbf{a})^2 = (\varepsilon_{12}^{cr})^2 + (\varepsilon_{23}^{cr})^2, \tag{118}$$

where $\mathbf{n} = \mathbf{e}_2$, $\boldsymbol{\beta} = \mathbf{I} - \mathbf{nn} = \mathbf{e}_1\mathbf{e}_1 + \mathbf{e}_3\mathbf{e}_3$, and the cartesian components refer to the coordinate system shown in Fig. 5. The strain in the direction of the fibers ε_n and the in-plane "volumetric" strain ε_p attain their maximum values at point A (see Fig. 5), which appears to be a possible site of fiber failure and debonding. Figures 9 and 10 show that the longitudinal (γ_n) and transverse (γ_p) shear stresses reach their maximum values on the surface of the hole.

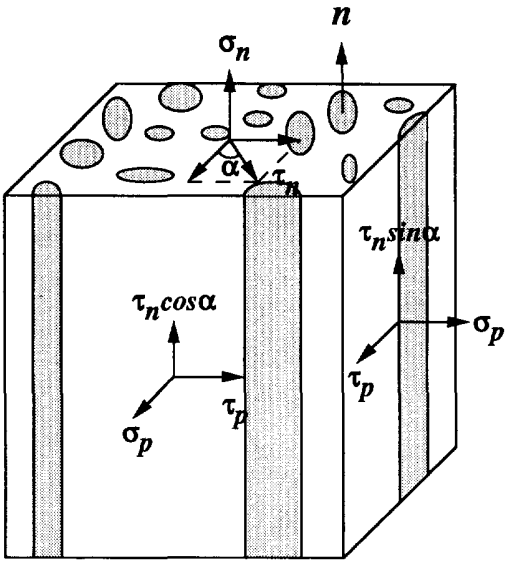

Fig. 10. Transversely isotropic stress invariants.

Acknowledgments—Fruitful discussions with Professors G. deBotton and P. M. Suquet are gratefully acknowledged. NA and CC acknowledge the support of the Office of Naval Research contract N00014-92-J-1808 through sub-agreement KK3006 from the University of California, Santa Barbara. PPC acknowledges the support of the NSF MRL Program at the University of Pennsylvania under Grant No. DMR-9120668. The ABAQUS finite element code was made available under academic license from Hibbitt, Karlsson and Sorensen Inc., Providence, RI.

REFERENCES

Aravas, N. (1992). Finite elastoplastic transformations of transversely isotropic metals. *Int. J. Solids Structures* **29,** 2137–2157.

Bakhvalov, N. and Panasenko, G. (1989). *Homogenisation: Averaging Processes in Periodic Media.* Kluwer Academic Publishers, Dordrecht, The Netherlands.

Christensen, R. M. (1979). *Mechanics of Composite Materials.* Wiley, New York, NY, USA.

deBotton, G. and Ponte Castañeda, P. (1993). Elastoplastic constitutive relations for fiber-reinforced solids. *Int. J. Solids Structures* **30,** 1865–1890.

Goto, S. and McLean, M. (1991a). Role of interfaces in creep of fibre-reinforced metal-matrix composites—I. Continuous fibers. *Acta Metall. Mater.* **39,** 153–164.

Goto, S. and McLean, M. (1991b). Role of interfaces in creep of fibre-reinforced metal-matrix composites—II. Short fibers. *Acta Metall. Mater.* **39,** 165–177.

Green, A. H. and Adkins, J. E. (1960). *Large Elastic Deformations.* Clarendon Press, Oxford, UK.

Hibbitt, H. D. (1984). ABAQUS/EPGEN—A general purpose finite element code with emphasis on nonlinear applications. *Nucl. Engng Des.* **77,** 271–297.

Jansson, S. (1992). Homogenized nonlinear constitutive properties and local stress concentrations for composites with periodic internal structure. *Int. J. Solids Structures* **29,** 2181–2200.

Johnson, A. F. (1977). Creep characterization of transversely-isotropic metallic materials. *J. Mech. Phys. Solids* **25,** 117–126.

Kelly, A. and Street, N. Creep of discontinuous fibre composites II. Theory for the steady state. *Proc. Roy. Soc. Lond.* A **328,** 283–293.

Lene, F. (1986). Damage constitutive relations for composite materials. *Engng Fract. Mech.* **25,** 713–728.

Lene, F. and Leguillon, D. (1982). Homogenized constitutive law for a partially cohesive composite. *Int. J. Solids Structures* **18,** 443–458.

Liu, I.-S. (1982). On representations of anisotropic invariants. *Int. J. Engng Sci.* **20,** 1099–1109.

McLean, M. (1985). Creep deformation of metal-matrix composites. *Compos. Sci. Technol.* **23,** 37–52.

McLean, M. (1988). Mechanisms and models of high temperature deformation of composites. *Mater. Res. Symp. Proc.* **120,** 67–79.

McMeeking, R. M. (1993a) Models for the creep of ceramic matrix composite materials, to appear.

McMeeking, R. M. (1993b). Power law creep of a composite material containing discontinuous rigid aligned fibers, to appear.

Mileiko, S. T. (1970). Steady state creep of a composite material with short fibres, *J. Mater. Sci.* **5,** 254–261.

Nagtegaal, J. D., Parks, D. M. and Rice, J. R. (1974). On numerically accurate finite element solutions in the fully plastic range. *Comput. Meth. Appl. Mech. Engng* **4,** 153–177.

Sanchez Palencia, E. (1980). *Non-homogeneous Media and Vibration Theory*, Lecture Notes in Physics, Vol. 127. Springer-Verlag, Berlin, Germany.

Smith, G. F. (1971). On isotropic functions of symmetric tensors, skew-symmetric tensors and vectors. *Int. J. Engng Sci.* **9,** 899–1916.

Suquet, P. M. (1982). *Plasticité et Homogénéisation*, Thèse de doctorat d'Etat, Université Paris VI.
Suquet, P. M. (1987). 'Elements of homogenization for inelastic solids', in *Homogenization Techniques for Composite Media* (Edited by E. Sanchez Palencia and A. Zaoui), Lecture Notes in Physics, Vol. 272, pp. 193–278. Springer-Verlag, Berlin, Germany.
Wang, C.-C. (1970a). A new representation theorem for isotropic functions: an answer to Professor G. F. Smith's criticism of my papers on representations of isotropic functions. Part 1. Scalar-valued isotropic functions. *Arch. Ration. Mech. Anal.* **36,** 166–197.
Wang, C.-C. (1970b). A new representation theorem for isotropic functions: an answer to Professor G. F. Smith's criticism of my papers on representations of isotropic functions. Part 2. Vector-valued isotropic functions, symmetric tensor-valued isotropic functions, and skew-symmetric tensor-valued isotropic functions. *Arch. Ration. Mech. Anal.* **36,** 198–223.
Weber, C. H., Löfvander, J. P. A. and Evans, A. G. (1993). The creep behavior of CAS/Nicalon continuous-fiber composites. *Acta Metall. Mater.* **41,** 2681–2690.

APPENDIX A

Transversely isotropic invariants

An alternative set of commonly used transversely isotropic invariants is

$$J_1 = \sigma_p = \tfrac{1}{2}\boldsymbol{\sigma} : \boldsymbol{\beta}, \tag{A1}$$

$$J_2 = \sigma_n = \boldsymbol{\sigma} : \mathbf{a}, \tag{A2}$$

$$J_3 = \tau_p^2 = \tfrac{1}{2}[(\boldsymbol{\sigma}\cdot\boldsymbol{\beta}) : (\boldsymbol{\sigma}\cdot\boldsymbol{\beta}) - \tfrac{1}{2}(\boldsymbol{\sigma} : \boldsymbol{\beta})^2], \tag{A3}$$

$$J_4 = \tau_n^2 = \boldsymbol{\sigma}^2 : \mathbf{a} - (\boldsymbol{\sigma} : \mathbf{a})^2, \tag{A4}$$

$$J_5 = \det(\boldsymbol{\sigma}), \tag{A5}$$

where $\mathbf{a} = \mathbf{nn}$, and $\boldsymbol{\beta} = \mathbf{I} - \mathbf{a}$. Physically, $(\sigma_p, \sigma_n, \tau_p, \tau_n)$ correspond to the in-plane hydrostatic stress, the longitudinal stress, the maximum transverse shear stress, and the resolved longitudinal shear stress, respectively. A schematic representation of the above invariants is shown in Fig. 10.

For convenience, we also define

$$\sigma_d^2 = (\sigma_p - \sigma_n)^2 = (\tfrac{3}{2}\mathbf{n}\cdot\boldsymbol{\sigma}'\cdot\mathbf{n})^2 \quad \text{and} \quad \sigma_s^2 = 3(\tau_p^2 + \tau_n^2), \tag{A6}$$

and note that

$$\sigma_e^2 = (\sigma_p - \sigma_n)^2 + 3(\tau_p^2 + \tau_n^2) = \sigma_d^2 + \sigma_s^2. \tag{A7}$$

If the fibers are aligned with the x_3 coordinate direction, i.e. $\mathbf{n} = \mathbf{e}_3$ and $\boldsymbol{\beta} = \mathbf{e}_1\mathbf{e}_1 + \mathbf{e}_2\mathbf{e}_2$, then

$$\sigma_p = \tfrac{1}{2}(\sigma_{11} + \sigma_{22}), \tag{A8}$$

$$\sigma_n = \sigma_{33}, \tag{A9}$$

$$\tau_p^2 = \sigma_{12}^2 + \tfrac{1}{4}(\sigma_{11} - \sigma_{22})^2, \tag{A10}$$

$$\tau_n^2 = \sigma_{13}^2 + \sigma_{23}^2, \tag{A11}$$

and

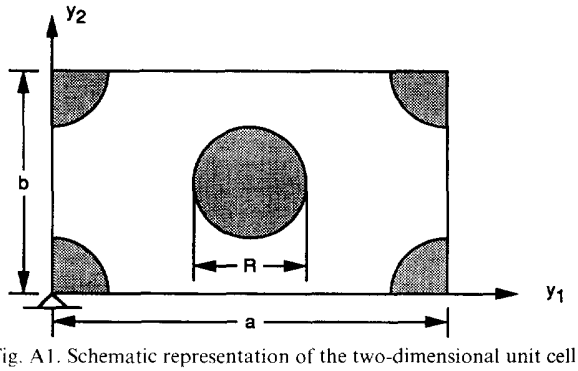

Fig. A1. Schematic representation of the two-dimensional unit cell.

$$\sigma_d^2 = (\tfrac{3}{2}\sigma'_{33})^2. \tag{A12}$$

In the following, we state the relationships between (I_1, I_2, I_4, I_5) and $(\sigma_p, \sigma_n, \tau_p, \tau_n)$:

$$\sigma_p = \tfrac{1}{2}(I_1 - I_4), \tag{A13}$$

$$\sigma_n = I_4, \tag{A14}$$

$$\tau_p^2 = \tfrac{1}{2}I_2 - I_5 + \tfrac{1}{2}I_4^2 - \tfrac{1}{4}(I_1 - I_4)^2, \tag{A15}$$

$$\tau_n^2 = I_5 - I_4^2, \tag{A16}$$

and

$$I_1 = \sigma_n + 2\sigma_p, \tag{A17}$$

$$I_2 = \sigma_n^2 + 2\sigma_p^2 + 2(\tau_p^2 + \tau_n^2), \tag{A18}$$

$$I_4 = \sigma_n, \tag{A19}$$

$$I_5 = \sigma_n^2 + \tau_n^2. \tag{A20}$$

APPENDIX B

The unit cell problem

We start with the case in which the unit cell occupies the region $0 \leqslant y_1 \leqslant a$, $0 \leqslant y_2 \leqslant b$, $-c \leqslant y_3 \leqslant c$, and then let $c \to \infty$.

For simplicity, we consider first the case in which there is no axial shearing, i.e. $E_{31} = E_{32} = 0$ and $\Sigma_{31} = \Sigma_{32} = 0$. The geometry of the unit cell and the applied loads are now symmetric with respect to $y_3 = 0$. Let $\mathbf{u}^{(1)}(\mathbf{y})$ be the solution for the Y-periodic field of the unit cell problem and define $\tilde{\mathbf{u}}(\mathbf{y})$ by

$$\tilde{u}_\alpha(y_1, y_2, y_3) = u_\alpha^{(1)}(y_1, y_2, -y_3), \tag{B1}$$

$$\tilde{u}_3(y_1, y_2, y_3) = -u_3^{(1)}(y_1, y_2, -y_3), \tag{B2}$$

where Greek subscripts range over the integers (1, 2). One can readily show that $\tilde{\mathbf{u}}(\mathbf{y})$ satisfies the governing equations and the boundary conditions (98)–(102), i.e. $\tilde{\mathbf{u}}$ is another solution of the unit cell problem. Since the solution is unique, this implies that $\tilde{\mathbf{u}} = \mathbf{u}^{(1)}$, i.e. $\mathbf{u}^{(1)}$ has the following symmetries:

$$u_\alpha^{(1)}(y_1, y_2, -y_3) = u_\alpha^{(1)}(y_1, y_2, y_3), \tag{B3}$$

$$u_3^{(1)}(y_1, y_2, -y_3) = -u_3^{(1)}(y_1, y_2, y_3). \tag{B4}$$

We therefore have

$$u_3^{(1)}(y_1, y_2, 0) = 0. \tag{B5}$$

When $c \to \infty$, there is no way to distinguish the location of $y_3 = 0$; hence, in view of the above symmetries, $\mathbf{u}^{(1)}$ must be independent of y_3, i.e.

$$u_\alpha^{(1)} = u_\alpha^{(1)}(y_1, y_2), \tag{B6}$$

$$u_3^{(1)} = 0. \tag{B7}$$

The solution of the unit cell problem can be now written as

$$\hat{u}_\alpha(y_1, y_2) = E_{\alpha\beta}y_\beta + u_\alpha^{(1)}(y_1, y_2), \tag{B8}$$

$$\hat{u}_3(y_3) = E_{33}y_3, \tag{B9}$$

which corresponds to a state of "generalized plane strain".

Referring to Fig. A1, we can arbitrarily set $\mathbf{u} = \mathbf{0}$ at $\mathbf{y} = \mathbf{0}$, which implies also that $\mathbf{u}^{(1)} = \mathbf{0}$ at $\mathbf{y} = \mathbf{0}$. Using eqn (B8) and taking into account the Y-periodicity of $\mathbf{u}^{(1)}$, we can readily show that

$$\hat{u}_\alpha(a, y_2) - \hat{u}_\alpha(0, y_2) = E_{\alpha 1}a \quad \text{and} \quad \hat{u}_\alpha(y_1, b) - \hat{u}_\alpha(y_1, 0) = E_{\alpha 2}b. \tag{B10}$$

The components of the macroscopic strain tensor $\mathbf{E}$ play the role of the "applied loads" for the unit cell problem. In order to impose eqn (B10) in a finite element computation, we introduce two fictitious nodes, say, M and N, and define the corresponding nodal displacement components as

$$\hat{u}_\alpha^M = E_{1\alpha}a, \quad \hat{u}_3^M = 0, \quad \text{and} \quad \hat{u}_\alpha^N = E_{2\alpha}b, \quad \hat{u}_3^N = 0. \tag{B11}$$

The conditions (B10) can be now written as

$$\hat{u}_\alpha(a, y_2) - \hat{u}_\alpha(0, y_2) = \hat{u}_\alpha^M \quad \text{and} \quad \hat{u}_\alpha(y_1, b) - \hat{u}_\alpha(y_1, 0) = \hat{u}_\alpha^N. \tag{B12}$$

The corresponding macroscopic stresses Σ_{ij} can be calculated as

$$\Sigma_{11} = \frac{F_1^M}{b}, \quad \Sigma_{12} = \frac{F_2^M}{b}, \quad \Sigma_{21} = \frac{F_1^N}{a}, \quad \Sigma_{22} = \frac{F_2^N}{a}, \tag{B13}$$

so that

$$(\boldsymbol{\Sigma} : \mathbf{E})(ab) = \mathbf{F}^M \cdot \hat{\mathbf{u}}^M + \mathbf{F}^N \cdot \hat{\mathbf{u}}^N, \tag{B14}$$

for all $\mathbf{E}$, where $\mathbf{F}^M$ and $\mathbf{F}^N$ are the nodal forces work conjugate to $\hat{\mathbf{u}}^M$ and $\hat{\mathbf{u}}^N$ at nodes M and N.

In a generalized plane strain calculation, the whole finite element mesh has one common degree of freedom in the y_3 coordinate direction. We assume that the mesh is of unit thickness in the y_3 direction and let $\hat{u}_3 = E_{33}$ be that common degree of freedom. Then the corresponding macroscopic stress component Σ_{33} is given by

$$\Sigma_{33} = \frac{F_3}{ab}, \tag{B15}$$

where F_3 is the nodal force conjugate to $\hat{u}_3$.

The conditions (B12) are enforced by using the so-called "multi-point constraints" in ABAQUS, which allows constraints to be imposed between different degrees of freedom in the model.

Depending on the problem under consideration, we prescribe the relevant components of $\mathbf{E}$ and $\boldsymbol{\Sigma}$, or equivalently of $\mathbf{F}^M$, $\mathbf{F}^N$ and $\mathbf{u}^M$, $\mathbf{u}^N$. For example, in the case of axial tension we let

$$E_{33} = \text{known}, \quad \text{and} \quad \Sigma_{11} = \Sigma_{22} = \Sigma_{12} = 0, \tag{B16}$$

or, equivalently,

$$\hat{u}_3 = E_{33} = \text{known}, \quad \text{and} \quad F_1^M = F_2^M = F_1^N = F_2^N = 0, \tag{B17}$$

and determine $\Sigma_{33} = F_3/(ab)$, and

$$E_{11} = \frac{\hat{u}_1(a, y_2) - \hat{u}_1(0, y_2)}{a}, \quad E_{21} = \frac{\hat{u}_2(a, y_2) - \hat{u}_2(0, y_2)}{a}, \tag{B18}$$

$$E_{12} = \frac{\hat{u}_1(y_1, b) - \hat{u}_1(y_1, 0)}{b}, \quad E_{22} = \frac{\hat{u}_2(y_1, b) - \hat{u}_2(y_1, 0)}{b}. \tag{B19}$$

The correctness of the numerical solution can be checked by verifying that $E_{11} = E_{22}$ and $E_{12} = E_{21} = 0$.

The generalized plane strain solutions are obtained by using four-node elements with 2×2 Gauss integration; an independent interpolation for the dilatation rate is used in order to avoid artificial constraints on incompressible modes (Nagtegaal *et al.*, 1974).

In the cases where there is axial shearing (i.e. $E_{31} \neq 0$ and/or $E_{32} \neq 0$), the unit cell problem is formulated in a similar way and the calculations are carried out by using a layer of eight-node three-dimensional brick elements with $2 \times 2 \times 2$ Gauss integration. The layout shown in Fig. 2 is repeated in the third direction to produce the aforementioned layer of three-dimensional elements.